Available online at www.CivileJournal.org

Civil Engineering Journal

(E-ISSN: 2476-3055; ISSN: 2676-6957)

Vol. 9, No. 11, November, 2023

Review Article

An Evaluative Review of Recycled Waste Material Utilization in High-Performance Concrete

Al Mashhadani D. A. Jasim [1, 2], Leong Sing Wong [1, 2*], Sih Ying Kong [3], Ahmed W. Al-Zand [4], Midhin A. K. Midhin [1, 2]

[1] *Department of Civil Engineering, College of Engineering, Universiti Tenaga Nasional, Jalan IKRAM-UNITEN, 43000 Kajang, Selangor, Malaysia.*

[2] *Institute of Energy Infrastructure, Universiti Tenaga Nasional, Jalan IKRAM-UNITEN, 43000 Kajang, Selangor, Malaysia.*

[3] *Discipline of Civil Engineering, School of Engineering, Monash University Malaysia, 47500 Bandar Sunway, Selangor, Malaysia.*

[4] *Department of Civil Engineering, Faculty of Engineering and Built Environment, Universiti Kebangsaan Malaysia, Bangi 43600, Selangor, Malaysia.*

Received 19 May 2023; Revised 18 October 2023; Accepted 23 October 2023; Published 01 November 2023

Abstract

The disposal of waste materials and their adverse effects on the environment have become a worldwide concern, disturbing the fragile ecological equilibrium. With growing awareness of sustainability in the construction industry, it is of great importance to recycle waste materials for producing high-performance concrete (HPC). This aligns with the twelfth Sustainable Development Goal (SDG) of the United Nations, emphasizing responsible production and consumption, especially concerning the production of HPC using waste materials and energy-efficient methods. The review evaluates the purposeful utilization of recycled waste materials to improve the engineering characteristics of HPC, taking into consideration pertinent literature. It encompasses a comparative evaluation of strength development, water absorption, microstructures, and x-ray diffraction (XRD) analyses of HPC manufactured with different types of recycled waste materials. The key result of the review showed that using incinerated bottom ash (IBA) below 25% and incorporating 40% copper slag can enhance HPC's mechanical performance. Additionally, recycled coarse aggregate (RCA) can replace up to 50% of conventional aggregate in self-compacting HPC with minimal impact on durability properties. In HPC cement substitution research, fly ash, silica fume, and metakaolin are prominent due to their availability, with fly ash showing remarkable durability when used as a 15% cement replacement. This thorough review offers valuable insights for optimizing the utilization of recycled waste materials in the development of environmentally friendly HPC.

Keywords: High-Performance Concrete; Energy-Efficient; Recycled Waste Materials; Strength Development; Water Absorption; Microstructures; X-Ray Diffraction.

1. Introduction

To ensure the sustainability of the world, the construction industry must embrace innovation and research to establish a circular economy [1]. Concrete, which stands as the predominant building material on a global scale [2-4], raises environmental concerns stemming from aggregate extraction and cement manufacturing, resulting in substantial energy consumption and significant carbon dioxide (CO_2) emissions [5-7]. To address environmental pollution effectively, it is imperative to implement sustainable approaches. These strategies encompass the valorization, recycling, and eco-friendly utilization of concrete waste by integrating it into cement or aggregates, thus helping to minimize adverse

* Corresponding author: wongls@uniten.edu.my

http://dx.doi.org/10.28991/CEJ-2023-09-11-020

impacts on the environment [8, 9]. Indeed, it is crucial to actively seek solutions for waste management, pollution control, resource preservation, and resource replenishment. In the construction sector, a substantial portion of waste originates from the demolition of buildings. The high costs associated with disposal, including dumping fees and landfill taxes, combined with the limited availability of disposal sites, present an opportunity for the development of high-performance concrete (HPC) that incorporates waste materials as a viable alternative.

HPC demonstrates its unique ability to meet precise performance and consistency standards that are challenging to achieve through conventional practices, which encompass traditional ingredients, mixing techniques, and curing methods. This carefully engineered concrete variant exhibits enhanced durability and, if desired, can surpass normal concrete in terms of strength. Due to its exceptional capacity to mitigate the adverse environmental impacts associated with the construction industry, HPC is gaining recognition as a powerful solution for sustainable building practices. This is primarily because it requires fewer cross-sections and subsequent maintenance compared to standard concrete [10, 11]. To fulfill specific structural and environmental project requirements, HPC employs materials like those in conventional concrete but with meticulously designed or engineered proportions. This meticulous approach ensures that HPC possesses outstanding mechanical, ductile, impact-resistant, and physical properties [12, 13], including reduced porosity, increased homogeneity, high toughness, and improved durability [14, 15]. However, a notable drawback of HPC is its higher cement demand compared to normal concrete [16, 17]. Several factors impact the environment, including extensive cement usage, which leads to CO_2 emissions, elevated production costs, and the depletion of natural resources [18, 19]. According to the guidelines outlined in ACI-363 [20, 21], high-strength concrete (HSC) is classified as concrete with a compressive strength exceeding 41 MPa. This specialized type of concrete finds widespread use in the construction industry, particularly in tall building projects, as it effectively reduces the dimensions of structural elements. Superplasticizers like sulphonated naphthalene formaldehyde and polycarboxylate superplasticizer are commonly employed to lower the water-to-binder ratio in concrete, thereby enhancing its strength. Concrete remains an indispensable construction material due to its accessibility, ease of molding, and ready availability [22-24].

The cement industry's energy consumption accounts for 12–15% of the total energy usage in the industry and contributes to 5–8% of global CO_2 emissions [25, 26]. Given the growing concerns regarding energy scarcity and the urgent issue of global warming, the exploration of low-carbon HPC has emerged as an intriguing area of research focus. The two primary goals of developing low-carbon concrete are to extend its service life using HPC and to substitute cement with low-carbon materials derived from industrial waste or by-products [27, 28]. The development of low-carbon concrete requires cooperation among regions and businesses because it is a locally sourced material. However, industrial waste materials (IWMs) generated during the production of goods present significant challenges in terms of processing, transportation, disposal costs, and environmental impact. Therefore, it is desirable to utilize IWMs in construction applications, particularly in cement concrete. These materials can function as complete or partial alternatives to cement, offering solutions to various issues associated with concrete. Special formulations of modern admixtures, derived from industrial waste, have been designed to interact optimally with concrete, addressing challenging aspects [29, 30]. It is recognized that the combination of industrial waste with regulated waste materials, such as fly ash, silica fume, and granulated blast furnace slag, can significantly enhance concrete properties. These waste components are commonly recycled in concrete production, offering the potential to improve economic viability, energy balance, and environmental impact [31, 32]. By incorporating a significant amount of reclaimed materials obtained from various industrial waste sources, the concrete sector not only has the potential to decrease landfill waste but also to support the attainment of the twelfth United Nations Sustainable Development Goal (SDG), which advocates for responsible production and consumption.

HPC has been extensively reviewed in several studies. These reviews focused on literature research of typical recycled raw material in HPC such as fibers [33-35], waste glass [36, 37], recycled aggregate [38-40], and palm oil fuel ash [41]. In addition, Tran et al. [42] reviewed the progressive research development of foam addition in lightweight HPC for improving the concrete's properties. The review primarily concentrated on the dynamics of foam deterioration, the latest advancements, emerging uses within the building and construction industries, and the possible obstacles in the development of foam-based concrete. In another review, Su et al. [43] observed a pivotal connection between the internal curing process and the porous structure of coral aggregate, impacting the durability of high-performance coral aggregate concrete (HPCAC). The review showed that the incorporation of supplementary cementitious materials has the potential to decrease chloride ion permeability in HPCAC by approximately 60%, and aggregate modification resulted in an approximate 20% enhancement in the cube compressive strength of HPCAC. Despite these reviews, there is currently a dearth of comprehensive review papers addressing the application of various types of recycled waste materials in HPC. Few literature comparisons have been made regarding the combined effects of these recycled materials on the enhancement of HPC's mechanical properties. To address these gaps in the literature, it is imperative to undertake a comprehensive review to assess the suitability of various types of recycled waste materials as partial substitutes for cement, fine aggregate, and coarse aggregate in HPC. This review article provides a complete understanding of how to optimize the use of waste materials in HPC effectively. It reveals valuable insights into identifying the most suitable combination of recycled waste materials for achieving optimal engineering performance in HPC. It provides a state-of-the-art analysis on the utilization of waste products such as incinerator bottom ash (IBA), crushed granite, powdered glass, rice husk ash (RHA), copper slag, ceramic waste powder (CWP), and others in sustainable high-performance

concrete (HPC) design. It presents a distinctive proposition regarding how these waste materials can be utilized to achieve robust bonds, fine pores, and enhanced mechanical resistance to withstand HPC loading failures. The objective of this review article is to comprehensively investigate and explore the engineering characteristics of HPC by incorporating a wide range of waste materials. The review is important because it gives an overview that by repurposing recycled waste materials in HPC, not only can the costs associated with disposing of recycled waste in landfills be reduced; but also, a more sustainable approach to concrete production can be fostered. Furthermore, this approach helps maintain ecological balance by ensuring a substantial presence of essential primary resources on Earth and transforming landfill sites into valuable locations for construction and development, rather than treating them solely as disposal sites. Overall, the comprehensive review that examines various combinations of recycled waste materials to enhance HPC properties can pave the way for more sustainable research into innovative waste materials with similar attributes, suitable for partial replacements of cement and aggregates in HPC. Figure 1 illustrates the flow chart that summarizes the methodology of the review article.

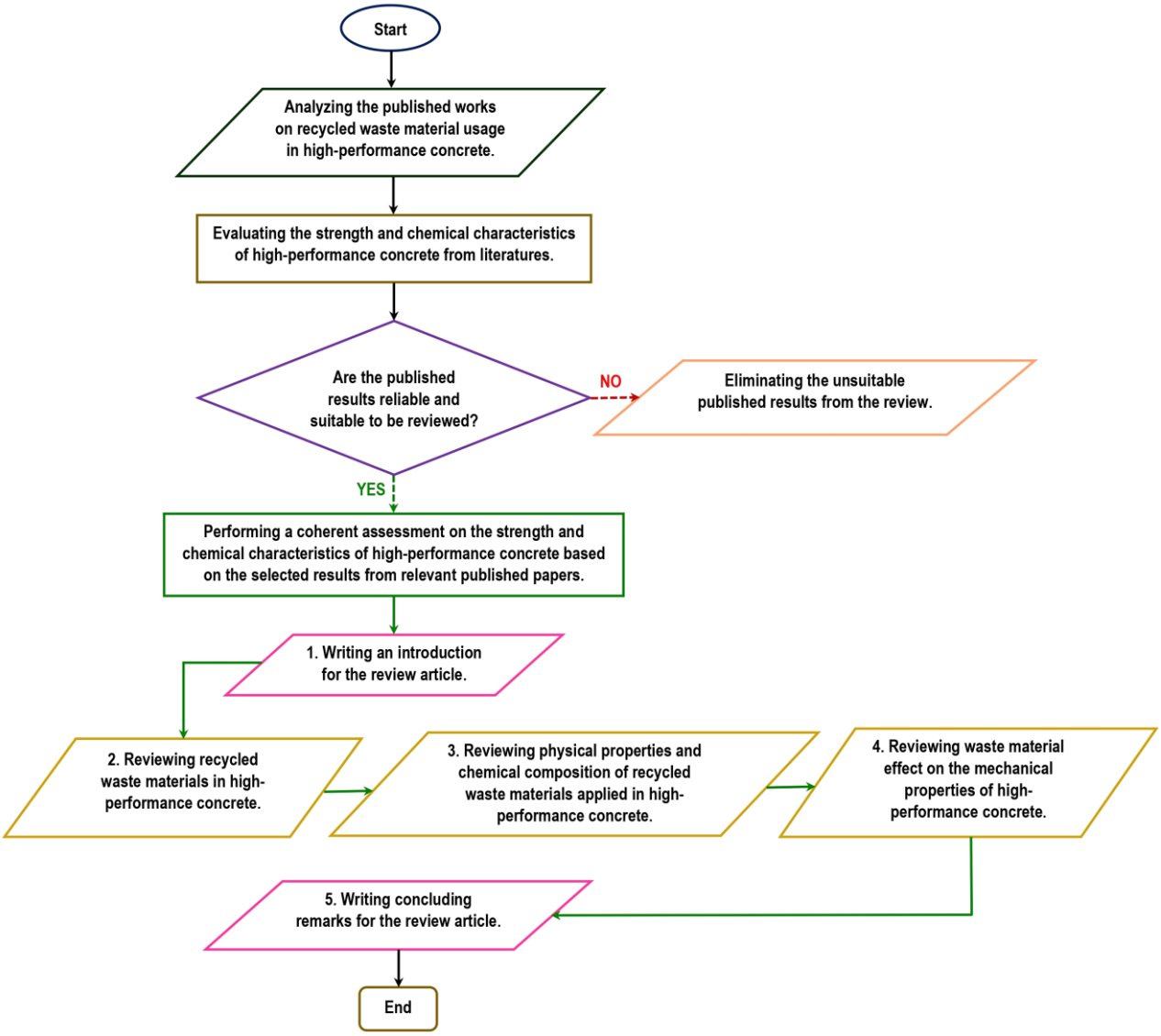

Figure 1. Flow chart that summarizes the methodology of the review article

2. Recycled Waste Materials in High-Performance Concrete

In recent times, there has been a notable surge in interest regarding the substitution of conventional resources with recycled waste materials in concrete. This attention stems from the vast potential it holds for fostering sustainable construction approaches and effectively tackling environmental apprehensions. By using recycled waste materials, the construction industry can reduce resource consumption, minimize waste generation, and decrease environmental impact. One common strategy involves replacing the cement in HPC with waste materials like blast furnace slag and silica fume. By incorporating this approach, it becomes possible to reduce the content of cement utilized in HPC without compromising or potentially improving its mechanical characteristics. Another aspect involves employing recycled aggregates as a replacement for natural aggregates in the production of HPC. Construction and demolition waste, such

as crushed rocks and demolished concrete, can be processed and repurposed as viable alternative aggregates. This not only decreases the demand for aggregates but also aids in diverting waste from landfills. Apart from cement and aggregates, waste materials can also be used as a replacement for other elements in the production of concrete. Large volumes of industrial waste materials or byproducts are produced annually in several industries in developing countries. Table 1 summarizes the types of recycled waste materials used as partial replacements for cement, fine aggregate, and coarse aggregate in HPC. Table 1 illustrates that it is possible to replace raw materials in HPC to a maximum extent ranging from 60 to 100% with recycled waste materials. For instance, two studies [25, 44] have reported the successful use of unprocessed waste fly ash, waste perlite powder, and waste cellular concrete powder to partially substitute cement, with replacements of up to 60%. The addition of a superplasticizer to the HPC mixtures made it possible to achieve high levels of cement replacement with recycled waste materials. The superplasticizer dispersed the cement and reduced the water content, thereby enhancing the self-compaction of HPC. Bottom ash and copper slag were applied up to full replacement of fine aggregate in HPC, as evident in the respective studies of Shen et al. [45] and Malkhare & Pujari [46]. Furthermore, Gonzalez-Corominas & Etxeberria [47] confirmed that coarse mixed recycled aggregate could be used to fully substitute the coarse aggregate in HPC. The composition of the coarse mixed recycled aggregate consists of 67.3% masonry products, 22.2% concrete products, 9.8% unbound aggregates, 0.1% glass products, and 0.7% other materials (such as wood, plastics, and gypsum). The effectiveness of recycled waste materials in replacing HPC aggregates depends on factors such as aggregate size, toughness, and packing efficiency.

Table 1. Various types of recycled waste material as partial replacements of cement, fine aggregate, and coarse aggregate in high-performance concrete

Reference	Recycled waste material	Conventional raw material in HPC	Replacement (%)
Gonzalez-Corominas & Etxeberria (2014) [47]	Coarse mixed recycled aggregate	Coarse aggregate	20 – 100%
Tahwia et al. (2022) [48]	Waste glass powder	Cement	10 – 50%
Amin et al. (2020) [49]	Ceramic waste powder	Cement	10 – 40%
Van Tuan et al. (2011) [50]	Rice husk ash	Cement	0 – 30%
Abed & Nemes (2019) [44]	Unprocessed waste fly ash	Cement	10 – 60%
Abdulkader & Nehme (2017) [25]	Waste perlite powder	Cement	10 – 60%
Abed & Nemes (2019) [44]	Waste cellular concrete powder	Cement	10 – 60%
Dixit et al. (2021) [51]	Biochar	Cement	Up to 30%
Davraz et al. (2018) [52]	Andesite Waste Powder	Cement	0 -20%
Xu et al. (2021) [53]	Ceramic Tile Waste Powder	Cement	15 – 55%
AlKhatib et al. (2020) [54]	Cement kilt dust	Cement	10 – 20%
Wang et al. (2018) [55]	Dehydrated cementitious powder	Cement	25%
Li et al. (2021) [56]	Waste basalt powder	Cement	Up to 15%
Yoo et al. (2021) [57]	Liquid crystal display	Silica flour	25 – 100%
Abdellatief et al. (2023) [58]	Granulated blast-furnace powder	Cement	30 – 50%
Sharma et al. (2016) [20]	Alccofine	Cement	15%
AlKhatib et al. (2020) [54]	Electric arc furnace dust	Cement	5 – 10%
Shen et al. (2020) [45]	Bottom ash	Fine aggregate	0 – 100%
Malkhare & Pujari (2018) [46]	Copper slag	Fine aggregate	10 - 100%
Yu & Wu (2020) [59]	Graphene oxide	Fine aggregate	0.06 wt%
Liu et al. (2020) [60]	Cathode ray tube glass	Fine aggregate	0 – 10%
Sharma et al. (2016) [20]	Foundry slag	Fine aggregate	10 – 45%
Suzuki et al. (2009) [61]	Waste porous ceramic	Coarse aggregate	0 – 40%
Abed & Nemes (2019) [44]	Recycled concrete aggregate	Coarse aggregate	0 – 50%
Afshinnia & Rangaraju (2016) [62]	Coarse glass aggregate	Coarse aggregate	20%

2.1. Recycled Waste Materials as a Partial Replacement of Cement in High-Performance Concrete

Tahwia et al. [48] embarked on research, focusing on examining the robustness of HPC by ingeniously introducing recycled waste glass powder (RWGP) as an alternative to quartz powder. The waste glass underwent meticulous grinding to achieve the exact powder size needed. A series of HPC mixtures were concocted in the study, ingeniously incorporating 10%, 30%, and 50% proportions of recycled RWGP as an inventive substitution for cement. Significant advancements were observed in the flexural and compressive strengths when 10% glass powder was utilized as a partial

replacement for cement in HPC. Van Tuan et al. [50] explored the impact of rice husk ash (RHA) on the mechanical properties of HPC. RHA is acknowledged for its exceptional specific surface area and concentration of amorphous silica (SiO_2), rendering it a dynamic pozzolan. The experiment was conducted to explore the incorporation of RHA as an alternative to cement in a concrete blend, accompanied by the inclusion of 10% silica fume (SF). The outcomes revealed that the combination of RHA and SF substantially bolstered the compressive strength of the concrete when compared to the control concrete specimen lacking RHA or SF. The decision to employ RHA was driven by its capacity to enhance specific characteristics of the concrete. In the published work of Amin et al. [49], the viability of utilizing ceramic waste powder (CWP) as a partial substitute for Portland cement in HPC mixtures was investigated, with replacement proportions ranging from 10% to 40%. Upon comparing the compressive strength of HPC mixtures with varying levels of CWP replacement after 28 days, it was observed that the highest compressive strength was exhibited by the control concrete specimen devoid of CWP. However, after 90 days, all concrete specimens displayed an accelerated rate of strength augmentation. The presence of CWP did not exert a significant influence on cement hydration when compared to concrete lacking CWP.

The effects of andesite waste powder (AWP) as a mineral additive in HPC were evaluated by Davraz et al. [52]. Concrete specimens were subjected to compressive strength testing at 28 and 90 days, and the results were compared with control specimens and specimens containing mineral additives. Among the C40 strength category, concrete specimens incorporating crushed waste ceramics (CWC) and finely ground fragments of tiles (FGT) demonstrated the highest compressive strengths at both 28 and 90 days when a substitution ratio of 10% was applied. Although the compressive strengths of CWC specimens were slightly lower than those of FGT specimens at substitution ratios of 15% and 20%, they were still superior to specimens containing silica fume (SF). A substitution ratio of 10% proved to be the most suitable for achieving maximum compressive strength in the C40 strength class, both at 28 and 90 days. In the case of the C55 strength class, the compressive strengths of concrete mixtures were evaluated after 28 and 90 days. Concrete specimens incorporating finely ground tile fragments (FGT) displayed the highest compressive strengths at both time points, with substitution ratios of 10% and 20%. At 90 days, the compressive strengths of FGT concrete specimens were comparable to those of the control mix for both 10% and 20% substitution ratios. In contrast, concrete specimens containing AWP generally exhibited higher compressive strengths than specimens with synthetic fine aggregates (SFA) at both 28 and 90 days. For the C55 strength class, the most favorable substitution ratios for AWP concrete specimens were determined to be 10% at 28 days and 20% at 90 days.

The potential utilization of various recycled waste materials in HPC was explored by Abed & Nemes [44]. These materials included recycled concrete coarse aggregate (RCA), unprocessed fly ash waste (UFAW), unprocessed perlite waste powder (UPWP), and ventilated concrete waste powder (VCWP). The study assessed the substitution of these recycled waste materials in concrete blends while maintaining a water-to-binder (w/b) ratio of 0.35 in self-compacting high-performance concrete (SCHPC). The substitution percentages ranged from 10 to 60%. The effect of steel fibers with different shapes and the replacement of 50% inert silica flour with waste glass powder from liquid crystal displays (LCD) on HPC strength development was examined by Yoo et al. [57]. Comparative analysis revealed that round fibers exhibited superior tensile and flexural characteristics, reduced matrix damage, and higher retreat energy compared to triangular fibers in HPC. Additionally, the twisting behavior observed in triangular fibers during torsional movement could potentially contribute to enhancing the performance and rupture behavior of HPC. The introduction of LCD glass powder significantly improved the tensile and flexural characteristics of HPC containing straight steel fibers. This improvement can be attributed to the increased frictional shear resistance observed at the interface between the fibers and the matrix. In the investigation carried out by Xu et al. [53], the utilization of ceramic tile waste powder (CTWP) in HPC was studied. It was discovered that the compressive strength of the concrete improved when the CTWP content reached 25%. The advantage in compressive strength was observed with CTWP contents below 45%, with the most significant improvement observed at CTWP compositions below 35%, resulting in a 10% difference in compressive strength for HPC. HPC incorporating 15, 25, and 35% CTWP exhibited enhanced compression and flexural behavior after 28 days. The large-scale use of CTWP as a replacement for cement can substantially reduce both the cost and environmental impact of HPC.

The impact of combining marine clay with biochar, a byproduct of wood biomass pyrolysis, on the strength development of HPC was investigated by Dixit et al. [51]. The study revealed that biochar has the potential to replace up to 30% of the cement weight in concrete while maintaining an acceptable level of compressive strength. However, all HPC specimens containing clay and biochar exhibited an approximately 10 to 12% lower 28-day compressive strength compared to the control concrete specimens. Wang et al. [55] and Qian et al. [63] observed the effects of replacing 25% of the original cement content with dehydrated cement powder (DCP) on the compressive strength development of HPC at various curing periods. Their findings showed a significant decline in the rate of compressive strength growth in HPC specimens after a 3-day curing period. In the study of Li et al. [56], the impact of using different types of basalt powder (BP) to partially replace the cement by 15% in the production of HPC was observed. The research findings indicated that as the content of basalt powder in HPC increases, the compressive strength gradually decreases. However, the use of finer basalt powder resulted in an improvement in the HPC's compressive strength. The desired HPC with high compressive strength was achieved with a 15% basalt powder content.

Abdellatief et al. [58] assessed the effectiveness of incorporating various industrial waste materials, including fly ash (FA), granulated blast furnace slag (GGBS), and silica fume (SF), as substitutes for cement in HPC. Multiple concrete mixtures were formulated using different combinations of Portland cement with GGBS (30–50%), FA (20–30%), or MK (15–25%). The findings revealed that the maximum values for both compressive strength and flexural strength of HPC were achieved when the replacement ratio of MK reached 15%. Sharma et al. [20] observed a significant enhancement in strength by incorporating alccofine (AF) as a partial substitute for cement in HPC. HPC specimens with varying proportions of AF (ranging from 0% to 20%) were produced, and the resulting compressive strength, flexural strength, and tensile strength after 28 days of curing were obtained after testing. The test results demonstrated that the highest levels of compressive strength, tensile strength, and flexural strength were achieved when 15% of Portland Pozzolana Cement (PPC) was replaced with AF in HPC.

The influence of three different curing methods, namely standard curing (SC), internal curing (IC) utilizing polyethylene glycol (PEG), and air curing (AC), on HPC mixtures was compared by Faried et al. [64]. The study also investigated the influence of four types of nanowaste materials, including ground nanometakaolin (NMK), waste glass (NWG), nano rice husk ash (NRHA), and chemically synthesized nano silica (NS). Various HPC mixes were prepared with dosages of 1%, 2%, and 3% of the nanomaterials. The findings revealed that incorporating 1% NS resulted in the highest strength for HPC across all curing conditions. Among the curing methods, AC exhibited the lowest strength for HPC. When comparing the addition of 1% NWG with 2 and 3% NWG, the inclusion of 1% NWG demonstrated the greatest strength for HPC. SC was identified as the most favorable curing method due to its cost-effectiveness, while AC yielded the lowest results with a slight increase in cost for HPC. Among the investigated nanowaste materials for HPC, 1% NMK exhibited the highest strength due to its compactness and strong hardening influence, which was comparable to blends with NS and NWG. AlKhatib et al. [54] produced HPC by combining nanosilica (NS) with two industrial wastes, namely cement kiln dust (CKD) and electric arc furnace dust (EAFD). The CKD (at percentages of 10, 15, and 20%) and EAFD (at 5 and 10%) were combined with 5% NS to replace the cement content in the concrete mix. In comparison to the control concrete specimen (Ordinary Portland cement - OPC), the CKD concrete exhibited lower compressive strength at all ages. However, the incorporation of NS led to enhanced compressive strengths for CKD concrete specimens with 10, 15, and 20% content. Furthermore, the addition of 5% NS to the concrete specimens containing 5 and 10% EAFD (Electric Arc Furnace Dust) resulted in a 28-day concrete compressive strength increase of 19.43 and 14.52%, respectively.

2.2. Recycled Waste Materials as a Partial Replacement of Fine Aggregate in High-Performance Concrete

Shen et al. [45] delved into the possibilities of employing reprocessed, fine material acquired from Incinerator Bottom Ash (IBA) in HPC. They extensively observed and evaluated its impact on the HPC's compression endurance over various durations of curing. Remarkably, their findings revealed that the inclusion of 25% IBA during the 28-day curing phase resulted in a subtle yet perceptible enhancement in the HPC's compressive strength. On the other hand, with the augmentation of IBA, the fortitude of HPC experienced a substantial deterioration. Astonishingly, when the entirety of IBA was utilized as a substitute, the HPC's strength plummeted by an extraordinary 20.9% in contrast to the control specimen. In a separate investigation by Malkhare et al. [46], the study showed a promising outlook on the feasibility of incorporating copper slag and other industrial residuals as alternatives to sand in HPC. Various quantities of copper slag, spanning from 0 to 100%, were skillfully employed to supplant the fine aggregate within the realm of HPC. The comprehensive investigation reached a resolute verdict, establishing that the augmentation of copper slag content and the replacement of 40% of the fine aggregate were instrumental in manifesting noteworthy enhancements across the board. Specifically, the compressive, split tensile, and flexural strengths of the resultant HPC surpassed those of the control specimen.

Yu and Wu [59] examined the effective utilization of graphene oxide (GO) in improving the properties of HPC incorporating fine recycled aggregate (RA). The study revealed that HPC containing fine RA exhibited mechanical strength, volume stability, and durability characteristics comparable to or even superior to HPC made with natural river sand. After considering crucial factors such as pore structure, durability, and mechanical properties in compression, tension, and flexure, the optimal dosage of GO was determined to be 0.06% by weight for the HPC. The study focused on testing various percentages of GO nanosheets, including 0.02, 0.04, 0.06, and 0.08 wt%, and concluded that 0.06 wt% yielded the most significant effects on the HPC. Discrepancies observed in the results could be attributed to variations in raw materials, admixtures, and water-cement-binder ratios across different studies. It is notable that previous research has shown that the inclusion of graphene oxide (GO) enhances cement hydration and improves the microstructure of cementitious materials.

In another discovery, Liu et al. [60] investigated the impact of Cathode Ray Tube (CRT) funnel glass, a potentially harmful waste material, on the application of HPC. The inclusion of this glass material enhances the mixture's flow characteristics, though it could potentially result in reduced compressive and flexural strengths. Nevertheless, it is important to highlight that HPC can fulfill the essential strength criteria for real-world applications even when utilizing CRT glass with a complete content of 100%. Sharma et al. [20] explored the use of foundry slag (FD) as a substitute for

traditional fine aggregates in HPC, contributing to its strengthening. It is possible to replace up to 45% of fine aggregates with FD in HPC. The compressive strength (CS) of all concrete mixtures exhibited a typical strength development pattern as the hardening age increased, indicating that replacing fine aggregates with FD did not have any detrimental effects.

2.3. Recycled Waste Materials as Partial Substitute of Coarse Aggregate in High-Performance Concrete

Suzuki et al. [61] meticulously assessed the intrinsic efficacy of recycled waste porous ceramic coarse aggregates (PCCA) in facilitating internal wet curing of HPC. The comprehensive analysis of the study encompassed six distinct variations of silica fume HPCs, both with and without the inclusion of PCCA. Their findings unequivocally demonstrated the remarkable effectiveness of PCCA in mitigating or eradicating autogenous shrinkage in HPCs featuring a low water-to-binder ratio of 0.15. Through the strategic integration of 40% PCCA, a ground-breaking breakthrough was achieved in the realm of non-shrinking HPC. Such advancement resulted in a substantial upsurge in compressive strength, accompanied by minimal internal stress. In an investigation by Afshinnia & Rangaraju [62], an in-depth exploration was undertaken to evaluate the feasibility of incorporating waste glass (WG) aggregates in the production of HPC. The investigation revealed that these WG aggregates exerted negligible influence on workability and only marginally diminished the overall strength of the concrete. Gonzalez-Corominas & Etxeberria [47] embarked on an exploration by integrating coarse mixed aggregates (CMA) derived from building demolition and ceramic waste substitution into the realm of recycled aggregate concrete. The experiments proved that employing up to 20% of CMA resulted in a commendable achievement, showcasing comparable compressive strength to that of conventional HPC with an impressive rating of 100 MPa. Collectively, these remarkable studies underscore the vast potential and myriad benefits of incorporating recycled materials into the production of HPC.

3. Physical Properties and Chemical Composition of Recycled Waste Materials Applied in High-Performance Concrete

Examining the physical properties and chemical composition of reused waste materials in HPC is essential, as there can be notable differences depending on the recycled material. Table 2 shows the details of the physical characteristics of the waste materials, including density, specific gravity, water absorption, and fineness modulus. To ensure optimal engineering properties of HPC, it is crucial to evaluate the diverse physical characteristics of the recycled waste materials before choosing the raw materials. Table 3 presents information regarding the chemical compositions of the fine recycled waste materials utilized as partial replacements for cement in HPC. The fine particles in these materials contain significant amounts of calcium oxide (CaO), silica (SiO_2), alumina (Al_2O_3), and iron oxide (Fe_2O_3). These elements are essential as they contribute to hydration and pozzolanic activities in the HPC admixtures, enabling the concrete to gradually strengthen during the curing process. Additionally, Tables 4 and 5 reveal the chemical compositions of the recycled waste materials employed as partial substitutes for fine and coarse aggregates in HPC, respectively. These waste materials consist of chemically inert coarse particles that effectively enhance the strength of HPC when utilized as aggregates.

Table 2. Physical properties of recycled waste materials used in high performance concrete

Material	Specific gravity (kg m^3)	Fineness modulus	Water Absorption (%)	Density (kg m^{-3})	Size (*u*m)	Blaine fineness (cm^2 g^{-1})	Crushing rate (%)
Porous ceramic waste [61]	2.27	6.66	9.31	-	-	-	21.4
Bottom ash [45]	-	-	7.4	2.10	-	2274.6	-
Copper slag [46]	3.74	2.89	1.40	-	-	-	-
Unprocessed fly ash [44]	-	-	-	2.15	-	4323	-
Waste perlite powder [25]	-	-	-	2.33	-	4159	-
Cellular concrete powder [44]	-	-	-	1.96	-	2513	-
Cathode Ray Tube glass [60]	-	-	-	2.916	-	-	24.8
Waste glass powder [48]	2.33	-	-	1.45	8	-	-
Alccofine [20]	2.9	-	-	0.6-0.7	-	-	-
Ceramic waste aggregate [49]	2.4	-	2	-	-	-	-
Blast furnace slag [58]	2.88	-	-	-	-	400	-
Foundry slag [20]	2.78	3	0.43	-	4.75	-	-
Coarse glass aggregate [62]	2.93	2.73	0.36	-	-	-	-
Coarse mixed aggregate [47]	-	-	16.45	1.8	-	-	34.6

Table 3. Chemical compositions of recycled waste materials for partial cement replacement in concrete (Weight %)

Material	CaO	SiO_2	Al_2O_3	Fe_2O_3	K_2O	MgO	Na_2O	SO_3	TiO_2	P_2O_5	CuO	V_2O_5	ZrO_2	LOI	Total (%)
Waste glass [62]	12.12	72.57	0.17	1.11	0.030	2.09	11.7	0.19	-	-	-	-	-	-	99.9
Rice husk ash [50]	1.39	92	0.23	0.21	2.99	0.36	0.2	1.42	-	-	-	-	-	-	98.8
Granulated blast furnace slag [58]	45.88	30.38	9.05	3.82	0.31	5.39	0.52	1.78	-	-	-	-	-	1.41	98.5
Andesite waste powder [52]	4.45	56.34	18.21	5.61	2.90	1.62	3.85	0.19	0.52	-	-	-	-	-	93.7
Unprocessed waste fly ash [44]	15.07	43.02	15.6	14.17	-	3.14	-	3.56	-	-	-	-	-	-	94.6
Waste perlite powder [25]	1.06	73.2	16.6	2.6	3.5	0.2	1.5	-	0.09	-	-	-	-	-	98.8
Waste cellular concrete powder [44]	22.81	54.28	5.09	2.16	-	1.15	-	4.90	-	-	-	-	-	-	90.4
Recycled waste glass powder [48]	9.8	74	1.8	0.4	0.56	1.2	11.6	-	0.04	-	-	-	-	0.6	100
Cement kiln dust [54]	49.3	17.1	4.24	2.89	2.18	1.14	3.84	3.56	0.34	0.12	0.029	0.013	0.011	15.8	100.6
Ceramic tile waste powder [53]	0.90	78.30	15.90	-	1.55	0.80	1.45	-	-	-	-	-	-	1.05	100
Marine clay [51]	0.24	55.74	32.48	2.45	2.35	2.43	0.71	-	3.6	-	-	-	-	-	100
Dehydrated cementitious powder [55, 63]	62.40	19.96	4.99	4.125	0.78	1.84	0.137	2.94	0.36	0.132	-	-	-	2.21	99.9
Tile ceramic waste [49]	16.12	54.2	16.21	5.79	-	-	-	-	-	-	-	-	-	-	92.3
Basalt powder [56]	14.84	48.71	14.58	4.90	1.83	2.76	3.45	1.62	-	-	-	-	-	-	92.7

Table 4. Chemical compositions of recycled waste materials for partial fine aggregate replacement in concrete

Material	CaO	SiO_2	Al_2O_3	Fe_2O_3	K_2O	MgO	Na_2O	SO_3	TiO_2	P_2O_5	CuO	PbO	BaO	Total (%)
Bottom ash [45]	17.3	49.60	11	5.36	1.63	2.09	6.04	1.15	-	-	-	-	-	94.17
Copper slag [46]	0.15	25.84	0.22	68.29	0.23	-	0.58	0.11	0.41	-	1.20	-	-	97.03
Graphene oxide [59]	67.45	6.46	7.25	3.73	-	1.14	-	12.32	-	-	-	-	-	98.35
Cathode ray Tube Glass [60]	2.1	55.6	3.6	0.1	6.1	2.0	2.0	-	0.1	-	-	22.3	4.0	97.9
Foundry slag [20]	33.6	31.4	8.20	18.20	-	1.94	-	0.22	-	-	-	-	-	93.56
Bottom ash [45]	17.3	49.60	11	5.36	1.63	2.09	6.04	1.15	-	-	-	-	-	94.17

Table 5. Chemical compositions of recycled waste materials for partial coarse aggregate replacement in concrete

Material	CaO	SiO_2	Al_2O_3	Fe_2O_3	K_2O	MgO	Na_2O	SO_3	TiO_2	P_2O_5	CuO	PbO	BaO	Total (%)
Coarse glass aggregate [62]	11.6	69.6	2.2	0.9	-	0.4	12.3	-	-	-	-	-	-	97.0

4. Recycled Waste Materials' Effect on the Mechanical Properties of High-Performance Concrete

4.1. The Mechanical Strength Development of High-Performance Concrete

Numerous empirical studies have extensively explored the effects of integrating recycled waste materials (RWM) into HPC as alternative substitutes for cement, fine aggregate, and coarse aggregate. In their comprehensive investigation, Tahwia et al. [48] conducted a series of tests and made noteworthy observations. It was discovered from the study that the inclusion of 10% glass powder (GP) as a cement substitute yielded remarkable flexural and compressive strengths in HPC, as outlined in Table 6. This notable strength enhancement can be attributed to the synergistic effect of silica fume and recycled waste glass powder (RWGP), which promoted an activated pozzolanic reaction. The interaction between the hydrated cement and RWGP led to the formation of calcium-silicate-hydrate (C-S-H) gel, effectively filling the voids and establishing a more compact microstructure within the concrete specimen. Initially, the incorporation of GP resulted in a decrease in concrete compressive strength after 28 days. However, over time, the strength rebounded significantly at 91 days due to the intensified pozzolanic reaction of GP, the utilization of calcium hydroxide (CH), and the production of additional C-S-H. However, when the GP percentage was increased to 15 and 20%, both the compressive and flexural strengths of HPC experienced a decline. Besides, a higher proportion of recycled glass powder led to a decrease in concrete density and absorption while concurrently increasing the permeability coefficient.

Table 6. Compressive strength of the control and optimized high-performance concrete (RWGP, RHA, and CWP) [48-50]

Waste recycled material	Concrete specimen	Compressive strength (MPa)
Recycled waste glass powder [48]	Control	180
	10% RWGP	210
Rice husk ash [50]	Control	172
	10% RHA	187
Ceramic waste powder [49]	Control	51.5
	10% CWP	50.1

In a study by Van Tuan et al. [50], experiments were conducted to investigate the use of rice husk ash (RHA) as a cement replacement along with 10% silica fume (SF) in HPC. The findings revealed a notable enhancement in the compressive strength of the HPC incorporating this combination, in contrast to the control concrete lacking both RHA and SF. The inclusion of RHA was driven by its potential to augment the characteristics of HPC. Intriguingly, when 20% of the cement was replaced with RHA, the compressive strength of the RHA concrete specimen outperformed that of the SF concrete specimen. Furthermore, the inclusion of both RHA and SF in the HPC specimens resulted in enhanced workability and compressive strength. Notably, a synergistic effect on compressive strength was observed when a combination of 10% RHA and 10% SF was utilized, as presented in Table 6. The incorporation of SF at a dosage of 25% contributed a significant amount of SiO_2, which effectively reduced interfacial gaps by interacting with portlandite [$Ca(OH)_2$], a byproduct of cement hydration.

Amin et al. [49] conducted a thorough investigation on the utilization of ceramic waste powder (CWP) as a partial substitute for Portland cement in HPC. The study explored various percentages of CWP substitution in HPC, ranging from 10% to 40%. Remarkably, the durability of CWP was found to be exceptional, establishing it as a promising alternative to cement in concrete applications. The compressive strength of HPC specimens with different levels of CWP replacement was evaluated at 28 days. The control concrete specimen, without CWP, exhibited the highest compressive strength during this period. However, an interesting trend emerged after 90 days, as all concrete specimens demonstrated an accelerated development in compressive strength. Surprisingly, the presence of CWP did not significantly impact cement hydration in HPC when compared to HPC without CWP. Notably, the control HPC, with its relatively high cement content, achieved the highest compressive strength value at 28 days, reaching an impressive 51.5 MPa, while a reduction in cement content led to a gradual decline in the 28-day compressive strength of HPC. The decline ranged from 15% for HPC-10 to 20% for HPC-40, as indicated in Table 6. Additionally, after a curing period of 90 days, a subtle acceleration in compressive strength enhancement was observed for all concrete specimens incorporating crushed waste porcelain.

Davraz et al. [52] investigated the effectiveness of mineral additives in improving the compressive strength of HPC specimens. The study compared HPC specimens containing mineral additives with control concrete specimens after 28 and 90 days of curing. The findings of the study revealed that in the C40 strength category, HPC specimens that incorporated crushed waste porcelain, andesite waste powder (AWP), and Tunçbilek Fly Ash (TFA) demonstrated the highest compressive strengths at both 28 and 90 days of curing, utilizing a 10% substitution ratio. Figure 2 is referred to for a visual representation of these results. Moreover, the compressive strengths of AWP concrete specimens were compared to those of concrete specimens with Seyitömer Fly Ash (SFA). The AWP concrete specimens showed slightly lower compressive strengths compared to the TFA concrete specimens at replacement ratios of 15% and 20%. Among the AWP concrete specimens, a 10% replacement ratio was identified as the optimal choice for achieving maximum compressive strength in the C40 strength category after both 28 and 90 days of curing.

To measure the performance of various concrete specimens within the C55 strength category, the compressive strengths were examined after 28 and 90 days of curing. The results indicated that when using substitution ratios of 10% and 20%, concrete specimens containing TFA displayed the highest compressive strengths at both time points. Notably, at 90 days of curing, the compressive strengths of TFA concrete specimens closely resembled those of the control concrete specimens for both 10% and 20% substitution ratios. In contrast, concrete mixtures incorporating AWP generally exhibited higher compressive strengths compared to concrete specimens with SFA at both 28 and 90 days of curing. Regarding the C55 strength category, the most favorable replacement ratios for AWP concrete specimens were determined to be 10% at 28 days of curing and 10% and 20% at 90 days of curing.

To evaluate the appropriateness of the mineral additives, the consideration was given to the combined amount of three main oxide compounds ($SiO_2 + Al_2O_3 + Fe_2O_3$). For class C supplementary additives, a minimum requirement of 50% was set, while for class F supplementary additives, it was 70%. According to ASTM standards, SFA and TFA had total major oxide contents of 84% and 88% respectively, classifying them as type F supplementary additives. The total major oxide content of AWP was determined to be 80%, which complied with the standards specified in TS EN 450. These standards mandate a minimum of 70% total major oxides for pozzolanic additives. Photomicrographs were employed to analyze the form and characteristics of the mineral additives at a microscopic level. Through examination of these images, it was observed that fly ashes showcased spherical and polished particles, contrasting AWP that comprised of asymmetrical particles with jagged contours.

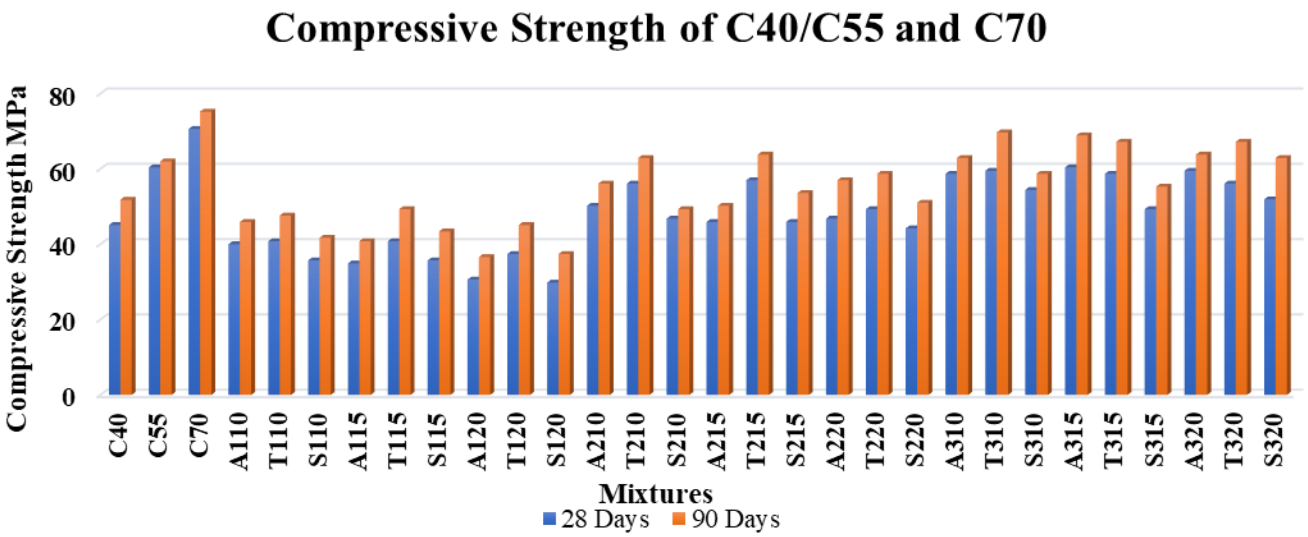

Figure 2. The compressive strength of HPC specimens. (Note: C, A, T, and S are the respective HPC specimens for control, andesite waste powder (AWP), Seyitömer Fly Ash (SFA), and Tunçbilek Fly Ash (TFA) at varying dosages under 28 and 90-day curing) [52].

Abed & Nemes [44] explored the potential utilization of various waste materials in high-performance concrete (HPC), including recycled concrete coarse aggregate (RCA), waste unprocessed fly ash (UWFA), waste unprocessed perlite powder (WPP), and waste ventilated concrete powder (WCCP). The research focused on assessing the replacement of these recycled waste materials in concrete mixes, maintaining a fixed water-to-binder (w/b) ratio of 0.35 in self-compacting high-performance concrete (SCHPC). The replacement percentages ranged from 10 to 60%. The study revealed that exceeding a 30% proportion of waste materials as a substitute for cement led to a decrease in the compressive strength of the concrete. However, the activation index, which measures the reactivity of the materials, demonstrated improvement over time at all levels of UWFA substitution for cement in the SCHPC. Furthermore, the results indicated that increasing the dosage of RCA significantly enhanced the concrete's compressive strength by up to 50%, as depicted in Figure 3. This improvement can be attributed to the enhanced roughness, porosity, and specific surface area of the recycled concrete aggregate (RCA) compared to the normal aggregate (NA) used in the SCHPC. These characteristics contribute to a stronger mechanical bond between the cement matrix and the recycled material in the SCHPC. It is crucial to recognize that the quality of RCA itself significantly affects the improvement of mechanical performance in recycled aggregate concrete (RAC), as depicted in Figure 3, in conjunction with other contributing factors.

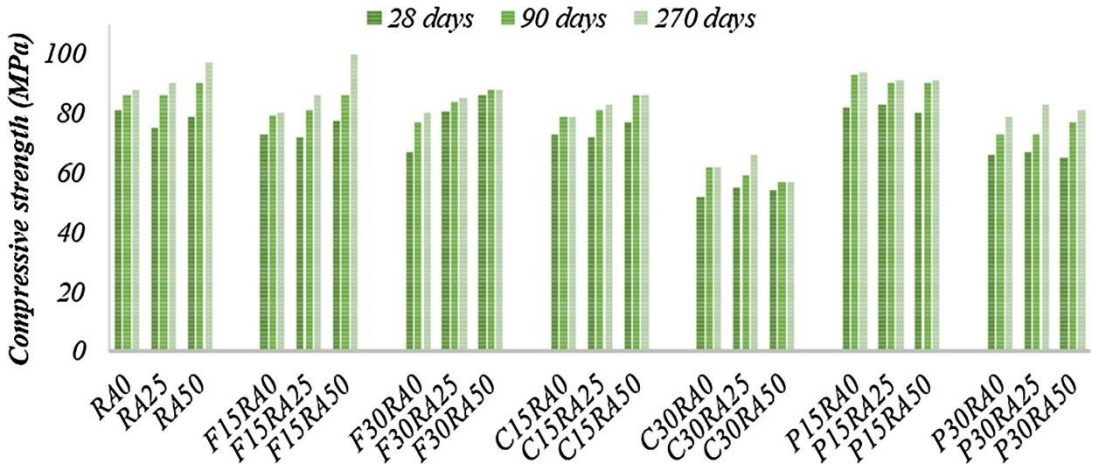

Figure 3. Compressive strength of HPC specimens of various mix designs (Note: RA is recycled aggregate, F- fly ash, C-cellular, p-perlite, at different percentages and curing) [44]

Yoo et al. [57] conducted a study where steel fibers were used and 50% of the silica flour of HPC was replaced with inert quartz. Waste glass powder material from liquid crystal displays (LCD) was utilized as an ingredient in the HPC. The research showed that round fibers exhibit better concrete tensile and flexural characteristics, reduced matrix damage, and higher retreat energy compared to triangular fibers. Other than that, the twisting behavior observed in triangular fibers during torsional movement may contribute to the enhanced performance and rupture behavior of HPC.

Incorporating waste glass powder from LCDs had no clear effect on the concrete's compressive strength when substituting 50% of the silica flour. This can be associated with the high packaging density of LCD glass waste powder in the HPC admixtures. The pozzolanic properties exhibited by LCD glass powder render it a fitting choice for augmenting the enduring compressive strength of typical concrete. The research findings point towards the capability of incorporating LCD glass waste powder, which not only enables the shaping of steel fibers but also retains or enhances the overall characteristics of the concrete.

In another research development, Xu et al. [53] studied HPC strength and observed an increment with extended curing durations while initially experiencing a decline with higher percentages of crushed tire waste powder (CTWP). The concrete compressive strength was found to rise when the CTWP content was at 25%, which can be considered the control group. It is evident that the concrete compressive strength advantage comes from a CTWP percentage of less than 45%. Specifically, when the composition of CTWP was lower than 35%, the early strength gain of HPC differed by 10%. HPC incorporating 15, 25, and 35% CTWP exhibited improved compression and flexural behavior after 28 days, as shown in Figures 4 and 5. Through the extensive utilization of CTWP as a partial substitute for cement, both the cost and environmental implications of HPC can be significantly mitigated. The superior compressive strength detected in concrete specimens containing CTWP can be credited to its pozzolanic characteristics, which facilitate the interaction with calcium hydroxide [$Ca(OH)_2$] and promote the hydration process of cement. This reaction fosters the generation of a greater amount of calcium silicate hydrate (C-S-H) gel. The presence of this gel aids in filling the voids and consequently leads to a more compact HPC mixture. As the content of C-S-H gel increases, the porosity reduces, culminating in an enhancement of the concrete's compressive strength.

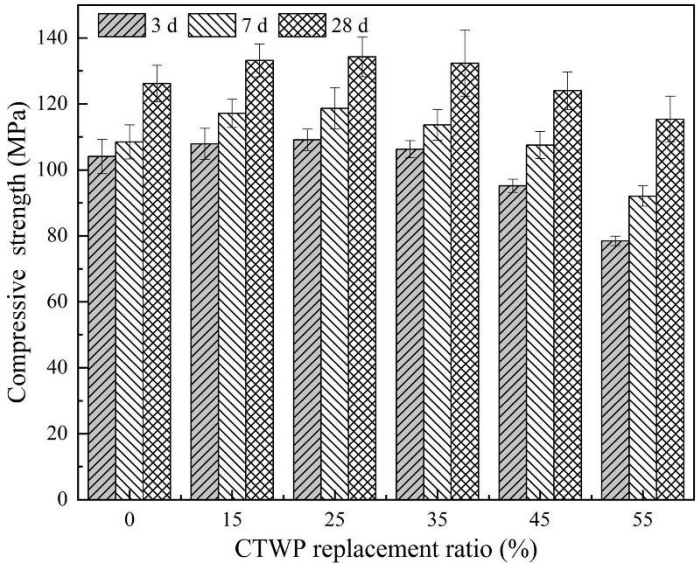

Figure 4. High-performance concrete compressive strength of different percentages of crushed tire waste powder (CTWP) [53]

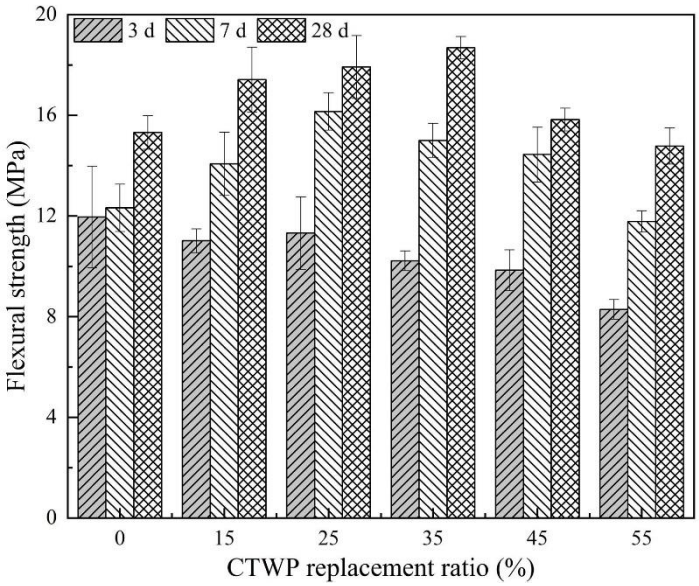

Figure 5. High-performance concrete flexural strength of different percentages of crushed tire waste powder (CTWP) [53]

Dixit et al. [51] observed that when marine clay is paired with biochar, a byproduct of wood biomass pyrolysis, biochar can replace 30% of the weight of cement in HPC. Nevertheless, it is worth noting that the compressive strength of all HPC specimens incorporating both clay and biochar experiences a slight decrease of approximately 10–12% when compared to the control concrete specimen. This reduction in concrete strength can be predominantly attributed to the relatively weaker nature of biochar particles, which act as vulnerable points within HPC due to their inferior strength in comparison to other components. The elastic modulus of the optimized HPC was measured to be 40 to 50 GPa, which is considerably high.

Wang and Qian et al. [55, 63] investigated the recycling of construction materials and the production of dehydrated cement powder (DCP) during the heat treatment process for HPC utilization. Gradually, up to 25% of the original cement content was replaced with DCP in the HPC. The study concentrated on the effects of DCP content on the development of compressive strength in HPC at different curing periods. The findings revealed that the rate of compressive strength growth in HPC specimens experienced a notable decline after a 3-day curing period. Initially, there is an upward trend in concrete compressive strength, followed by a subsequent decrease after 7 days of curing. This behavior facilitates the polymerization of oligomers in the HPC when the DCP undergoes rehydration, which typically happens seven days after curing once a specific polymerization stage is completed.

Li et al. [56] explored the potential for recycling broken stones and rock flour from tunnel waste to produce artificial sand, which generates a range of by-products called rock flour for usage in HPC (Figure 6). Three different types of leftover basalt powder (BP) were used to partially replace the cement by 15% in producing HPC. The findings indicate that as the content of basalt powder in the HPC increased, the compressive strength gradually decreased. However, when finer basalt powder was used, the HPC's compressive strength improved. The desired HPC achieved high compressive strength with a 15% basalt powder content, particularly using BP3 with fine particles and autoclave curing, as shown in Figure 4. The research suggests that heat curing can be effectively employed to create environmentally friendly HPC. Although the compressive strength of HPC specimens without basalt powder experienced a marginal decline in contrast to the control concrete specimen during standard curing conditions, the addition of basalt powder to HPC specimens resulted in enhanced compressive strength following exposure to heat curing, steam curing, and autoclave curing

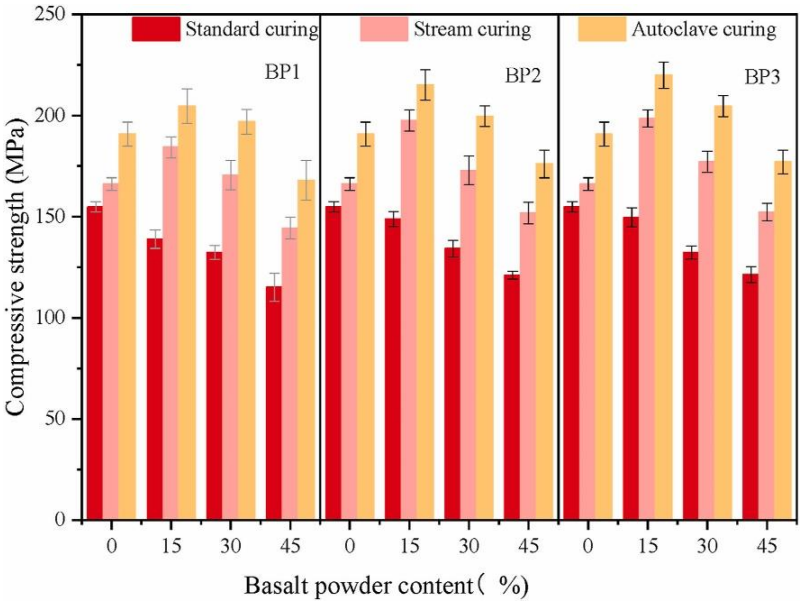

Figure 6. Compressive strength of HPC specimens incorporating basalt powder subjected to heat curing, steam curing, and autoclave curing [56]

Abdellatief et al. [58] formulated multiple concrete mixtures by combining Portland cement with ground granulated blast furnace slag (GGBS) powder (30–50%), fly ash (FA) (20–30%), or metakaolin (MK) (15–25%). According to the results, Figure 6 illustrates the highest recorded values for compressive strength, flexural strength, and splitting tensile strength of the HPC when the replacement ratio of MK reached 15%. Remarkably, in comparison to the control concrete, there were notable enhancements in compressive strength at various time intervals. Specifically, improvements of 10.2, 6.43, and 3.7% were observed at 3, 7, and 28 days, respectively. Furthermore, the concrete flexural strength exhibited improvements of 4.61 and 5.62% at 28 and 90 days, as shown in Figure 7, with incremental gains of 4.95 and 3.7% observed every 90 days.

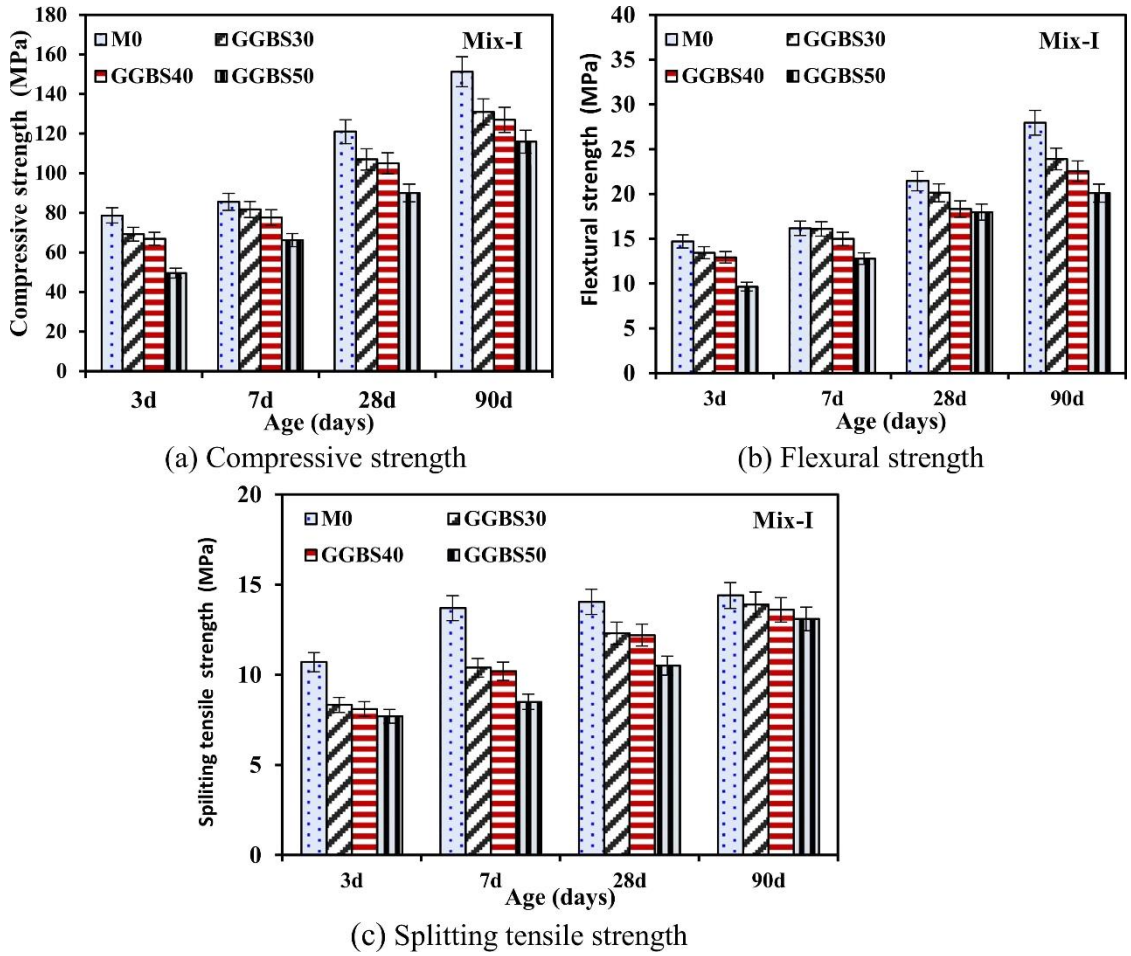

Figure 7. Compressive strength, flexural strength, splitting tensile strength of HPC specimens enhanced with metakaolin (MK) [58]

Sharma et al. [20] observed a noticeable enhancement in strength when alccofine (AF) was partially substituted for cement in HPC. HPC specimens were fabricated with varying proportions of AF, ranging from 0 to 20%. After 28 days of curing, the resulting compressive strength (CS), tensile strength (TS), and flexural strength (FS) were determined and shown in Table 7. Following the 28-day curing period, the test results were analyzed, and the HPC specimens with different percentages of AF were compared based on CS, TS, and FS, according to the requirements specified in the Indian Standard. The results indicate that the highest levels of CS, TS, and FS were achieved when 15% of Portland Pozzolana Cement (PPC) was replaced with AF in HPC. This suggests that 15% is the maximum dosage of AF for the HPC. By utilizing the appropriate amount of AF as a partial cement replacement, not only was the chloride ion permeability reduced, but the strength of the concrete was also improved.

Table 7. Compressive strength, flexural strength, and tensile strength of 0 to 20% alccofine high-performance concrete [20]

Alccofine (%)	Compressive Strength28-day (MPa)	Tensile Strength 28-day (MPa)	Flexural Strength 28-day (MPa)
0	79.56	5.270	7.335
5	83.64	6.302	7. 82
10	85.39	6.729	8.964
15	102.32	7.271	10.325
20	92.39	7.024	10.156

Faried et al. [64] analyzed the impact of four distinct types of nano waste materials, including ground nano metakaolin (NMK), nano waste glass (NWG), nano rice hull ash (NRHA), and chemically produced nano silica (NS), on HPC. Various HPC mixes were formulated, integrating 1%, 2%, and 3% dosages of the nanomaterials. Notably, the inclusion of 1% NS exhibited the highest concrete strength under all curing conditions. The reason behind this phenomenon can be credited to the existence of intricate silica structure and its significant contribution to promoting the breakdown of calcium silicate hydrate (C-S-H) compounds. The effectiveness of this interaction is influenced by the filling and pozzolanic actions of the nanoparticles (NPs) introduced through NS supplementation of the HPC. Among the curing procedures, autoclave curing (AC) provided the lowest concrete strength. Comparing 2 and 3% NWG, the addition of 1% NWG exhibited the greatest strength in concrete. Steam curing (SC) was found to be the most favorable curing method for HPC due to its cost-effectiveness, while AC yielded the lowest results with a slight increase in cost. Among the investigated nano waste materials, 1% NMK showed the greatest strength of concrete due to its compactness

and strong hardening influence, comparable to blends with NS and NWG. The convergence of the concrete strength curves was observed at 2% for SC and 3% for immersion curing (IC). The optimal dosage of NRHA, which exhibited its highest compressive strength in HPC, was determined to be 3% due to its porous characteristics facilitated by NWG-induced pore formation. The inclusion of nanoparticles (NPs) clearly improves the compressive strength of HPC, with 1% NS, 1% NWG, and 1% NMK being particularly effective and exhibiting optimal strengths due to the compactness of the concrete specimens. In comparison to IC and AC, SC demonstrated higher rates of concrete strength enhancement with NWG, NRHA, NMK, and NS, reaching 12, 20, 9, and 11%, respectively, while the rates decreased to 5, 19, 6, and 3% under AC.

In a published work by AlKhatib et al. [54], a synergistic approach was employed to investigate the combined usage of nanosilica (NS) with two industrial by-products, namely cement kiln dust (CKD) and electric arc furnace dust (EAFD), as supplementary cementitious materials in HPC. CKD was incorporated at varying proportions of 10, 15, and 20%, while EAFD was utilized at 5 and 10%, both in conjunction with 5% NS, to partially replace the cement content in the concrete. A comparative analysis with the control concrete, which utilized ordinary Portland cement (OPC), consistently exhibited lower compressive strength in the CKD concrete across all time periods. However, the incorporation of NS resulted in a remarkable enhancement of the compressive strength in CKD and EAFD concrete specimens, as clearly depicted in Figures 8 and 9. The addition of NS exerted a positive influence on the compressive strengths of CKD mixtures containing 10, 15, and 20% CKD content (Figure 8). Moreover, the inclusion of 5% NS in the concrete mixture comprising 5% and 10% EAFD yielded a significant increase of 19.43 and 14.52%, respectively, in the 28-day compressive strength compared to OPC concrete (Figure 9). Notably, the most substantial improvement in compressive strength was observed when utilizing concrete with 10% EAFD and incorporating 5% NS.

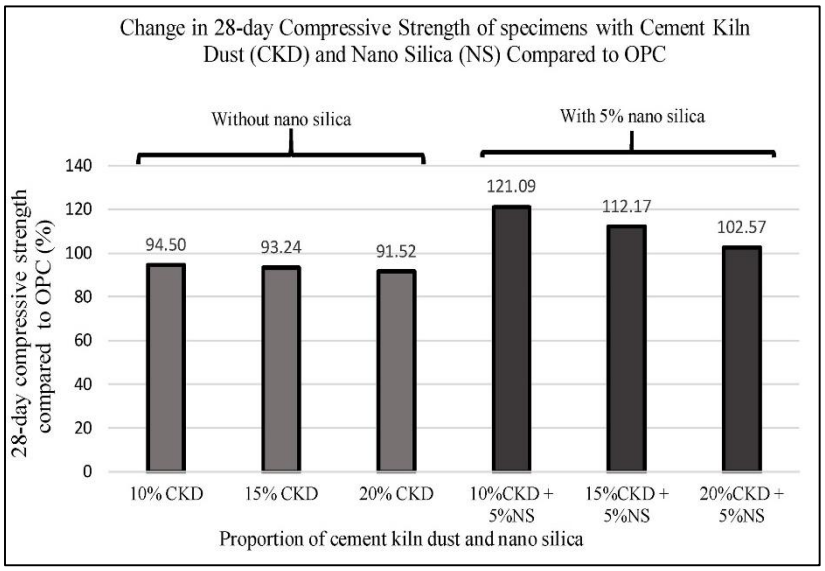

Figure 8. A comparison between cement kiln dust concrete specimens' compressive strength and the strength of OPC concrete [54]

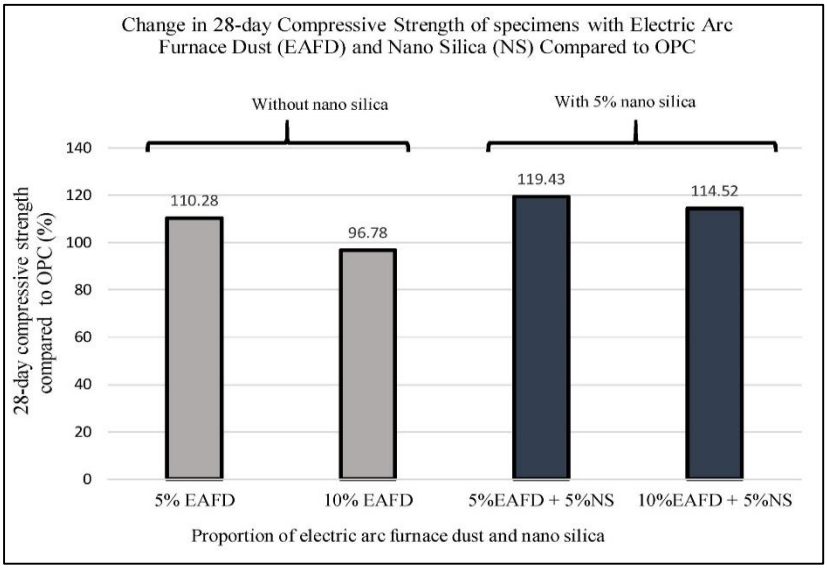

Figure 9. Electric arc furnace dust concrete specimens' 28-day compressive strength in comparison to that of OPC concrete [54]

Shen et al. [45] examined the influence of incorporating recycled fine aggregate derived from incinerator bottom ash (IBA) in HPC and evaluated its impact on compressive strength at different curing periods. It was noted that the introduction of 25% IBA during the 28-day curing period led to a slight improvement in the compressive strength of HPC. However, as time progressed, the strength of the concrete exhibited a significant decline with the inclusion of IBA. When the replacement ratio of IBA reached 100%, the compressive strength of HPC decreased by more than 20.9% compared to the control concrete. The observed enhancement in concrete compressive strength upon the addition of IBA can be attributed to its internal curing action, which shares similarities with the internal curing effect observed with lightweight aggregates. Previous research suggests that when the percentage of IBA is low, the beneficial impact of internal hardening on concrete compressive strength may outweigh the adverse effects caused by the porous nature of IBA.

Malkhare et al. [46] emphasized the potential of using copper slag and other industrial by products as alternatives to sand in HPC. Different proportions of copper slag, ranging from 0 to 100%, were utilized as replacements for fine aggregate in the concrete specimens. The findings of the study indicated that increasing the amount of copper slag in the concrete mixes had a notable and positive influence on workability and density. Moreover, the research demonstrated that substituting 40% of the fine aggregate with copper slag resulted in significant improvements in compressive, split tensile, and flexural strength compared to the control concrete. The improved concrete exhibited remarkable strength enhancements of up to 60% when compared to the control concrete. However, as the replacement rate reached beyond 60%, a decline in concrete strength was observed due to the increase in the free water content of the mixture. Additionally, the utilization of copper slag as a fine aggregate replacement led to reduced production costs for concrete, making it a cost-effective option.

Yu & Wu [59] demonstrated the effective utilization of graphene oxide (GO) in improving the properties of HPC incorporating fine recycled aggregate (RA). The investigation indicated that HPC incorporating fine recycled aggregates (RA) exhibited mechanical strength, volume stability, and durability characteristics comparable to, or even surpassing, HPC made with natural river sand. By considering essential factors such as pore structure, durability, and mechanical properties in compression, tension, and flexure, the optimal dosage of graphene oxide (GO) in the concrete was determined to be 0.06% by weight. The study conducted tests using various percentages of GO nanosheets, including 0.02 wt%, 0.04 wt%, 0.06 wt%, and 0.08 wt% (Figure 10), and concluded that 0.06 wt% yielded the most significant impact on concrete strength. Drawing from prior research, the addition of graphene oxide (GO) has been demonstrated to enhance cement hydration and improve the microstructure of cementitious materials. This phenomenon likely contributes to the observed increase in compressive strength of the concrete in the study. Additionally, the inclusion of GO leads to modifications in cement hydration products, further contributing to the positive effects on HPC.

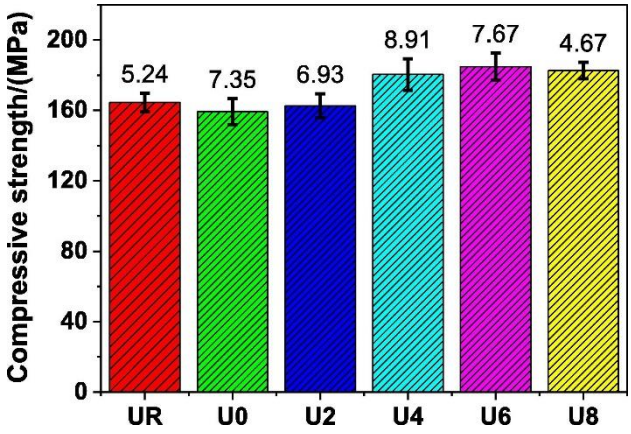

Figure 10. Compressive strength of HPC using different percentage of graphene oxide (GO) [59]

Liu et al. [60] emphasized the potential risks posed by cathode ray tube (CRT) funnel glass, a hazardous waste primarily due to its lead content, to human health and the environment. However, its integration into HPC enhances the mixture's flow characteristics, albeit at the expense of reduced compressive and flexural strengths. It is important to underline that HPC can meet the essential strength criteria for real-world applications, even with a complete 100% incorporation of CRT glass. The reduction in mechanical strength of HPC when utilizing CRT glass can be attributed to several factors like increased porosity, a lesser extent of cement hydration, and weaker bond strength compared to the interfacial transition zone (ITZ). Notwithstanding the observed decline, the research showcases a feasible approach to recycling hazardous waste CRT for HPC application. This solution presents a practical alternative that allows for freely adjustable replacement ratios and alleviates safety concerns.

It was experimentally proven by Sharma et al. [20] that replacing traditional fine aggregates in concrete with foundry slag (FD) contributes to its strengthening. The study revealed that it is possible to replace up to 45% of fine aggregates with FD in HPC. The compressive strength of all concrete mixtures exhibited a typical strength development pattern as the hardening age increased, indicating that replacing fine aggregates with FD did not have any detrimental effect. By

identifying the optimal dosage of fine and well-distributed airborne fine particles (AF), superior early strength of HPC was obtained compared to other pozzolanic materials and silica fume. The fine nature and treated particle size distribution of AF promoted its pozzolanic reaction, resulting in improved pore structure through hydration and enhanced packing of the concrete. Table 8 provides evidence of the enhanced mechanical properties of the concrete resulting from the incorporation of FD. The substantial SiO_2 concentration in FD, coupled with its interaction with $Ca(OH)_2$, facilitated the generation of supplementary C-S-H gel, ultimately leading to a notable improvement in concrete compressive strength. It is worth noting that the presence of unbound chloride ions can exert an influence on the strength attributes of the concrete. In summary, the utilization of FD and AF in concrete exerts a favorable influence on its mechanical attributes, pore structure, and strength characteristics.

Table 8. Compressive, flexural, and tensile strength of high-performance concrete with 45% foundry slag (FD) [20]

Strength test	Concrete specimen	28-day strength (MPa)
Compression	CTR	102.32
	F45	105.72
Tensile	CTR	7.271
	F45	7.393
Flexural	CTR	10.325
	F45	12.464

Suzuki et al. [61] delved into the utilization of recycled waste porous ceramic coarse aggregates (PCCA) in HPC specimens. The primary objective was to enhance cement hydration and mitigate autogenous shrinkage in HPC. The outcomes of the study showcased promising potential for the application of recycled porous ceramic waste as pre-saturated porous coarse aggregates, effectively serving the purpose of internal wet curing in HPC. Other than that, the incorporation of these aggregates into HPC specimens demonstrated an effective reduction in autogenous shrinkage. The successful reduction of early-age cracking and autogenous shrinkage in high-performance silica fume concrete can be attributed to the utilization of varying amounts of pre-saturated PCCA for internal water curing. Moreover, the inclusion of PCCA for internal water curing offers an added advantage by enhancing the cement hydration reaction, leading to a great improvement in compressive strength beyond the reduction in autogenous shrinkage. Notably, the HPC specimen containing PCCA exhibited a remarkable increase of approximately 10 to 20% in compressive strength at 28 days, as convincingly demonstrated in Figure 11.

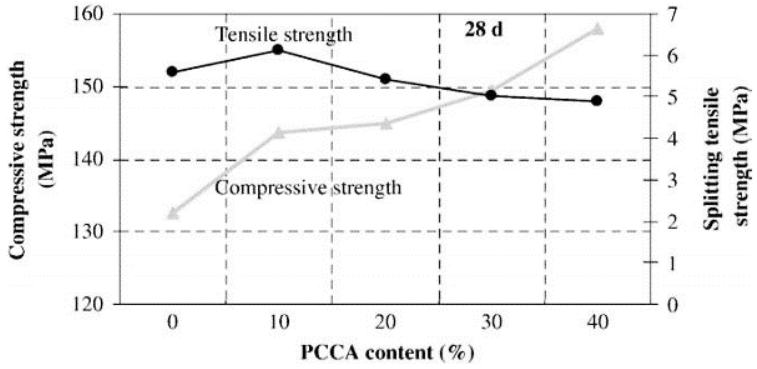

Figure 11. The 28-day compressive and splitting tensile strength development versus porous ceramic waste aggregates (PCCA) proportions of HPC [61]

To comprehensively explore the substitution of natural coarse aggregates, a thorough investigation was carried out by Gonzalez-Corominas & Etxeberria [47]. Their extensive study focused on HPC and involved the incorporation of different proportions (20, 50, and 100%) of coarse mixed aggregates (CMA). The main objective was to assess and compare the physical, mechanical, and durability properties of recycled aggregate concrete with those of conventional control concrete. The findings revealed that incorporating up to 20% CMA led to a comparable compressive strength of 100 MPa, which is similar to that of conventional HPC. However, surpassing the threshold of 20% CMA resulted in a decline in compressive strength when compared to the control concrete. This reduction in strength was attributed to the relatively lower toughness exhibited by CMA in contrast to natural aggregates. Remarkably, the CMA exhibited a significantly higher crushing aggregate value, which can be attributed to their larger nominal size.

Leng et al. [65] researched the influence of carbonated recycled coarse aggregate (CRCA) on the strength gain of HPC specimens. In the research work, recycled coarse aggregate (RCA) was produced by crushing waste concrete from abandoned bridges. The RCA was then subjected to a 24-hour carbonization treatment to yield CRCA. Figure 12 depicts the results that show the influence of natural aggregate (NA), RCA, and CRCA and curing duration on the compressive

strength of HPC specimens. Regardless of the curing duration, the HPC specimens with CRCA were tested to have the highest compressive strength compared to those with NA and RCA. The compressive strength values of the HPC specimens with CRCA were found to be 5.0, 6.5, and 9.1% higher than NA at the respective 3, 7, and 28-day curing times, respectively. The reason for this can be attributed to CRCA, which has fewer pores compared to RCA and NA. This resulted in lower water absorption by HPC specimens, thus enhancing their robustness. Other than that, CRCA can generate nano-calcium carbonate and silica on its surface, potentially promoting cement hydration on the RCA's surface and strengthening the bonding strength at the interface among CRCA, cement, and other raw materials [66, 67].

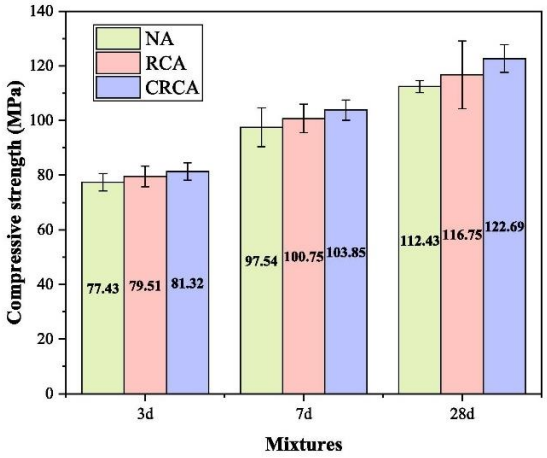

Figure 12. Influence of natural aggregate (NA), recycled coarse aggregate (RCA), and carbonated recycled coarse aggregate (CRCA) and curing duration on the compressive strength of HPC specimens [65]

4.2. Water Absorption of High-Performance Concrete Improved with Recycled Waste Materials

The water absorption of HPC typically exhibits a lower value compared to conventional concrete, although it can vary depending on the specific mix design and other factors. This enhanced performance can be attributed to the integration of specialized additives and superior-quality materials in the formulation, which contribute to the formation of a more compact and impermeable structure in the concrete. Numerous factors influence the water absorption of concrete, including the water-to-cement (w/c) ratio, curing techniques, concrete age, compaction methods, and aggregate characteristics. Figure 13 provides a visualization of the water absorption behavior of HPC after a 28-day curing period. For instance, the water absorption levels of different concrete specimens incorporating recycled waste glass powder (RWGP), such as RWGP Ref., 90 C/10RWGP, 70 C/30RWGP, 50 C/50RWGP, 75QP/25RWGP, 50QP/50RWGP, and 0QP/100RWGP, were measured at 0.7%, 0.65%, 0.5%, 0.35%, 0.6%, 0.55%, and 0.45%, respectively [68]. Notably, an increase in the RWGP content resulted in a reduction in the water absorption of HPC. This decrease can be attributed to the pozzolanic reaction triggered by RWGP, leading to the formation of calcium-silicate-hydrate (C-S-H) gel, which aids in pore sealing and enhances the microstructure of HPC [69]. The water absorbance of HPC was also influenced by the surface properties of the glass powder. As the HPC gradually replaced cement with glass powder, the water absorption decreased over time. The decline was influenced by factors such as the evolving density of the concrete specimen, the condition of the glass powder's surface, and the progress of the hydration process [70]. By solely substituting cement with glass powder, the HPC exhibited reduced porosity and enhanced compactness, resulting in lower water absorption. Increasing the glass powder content by 20% in the HPC led to a twofold reduction in water absorptivity compared to the control concrete [69].

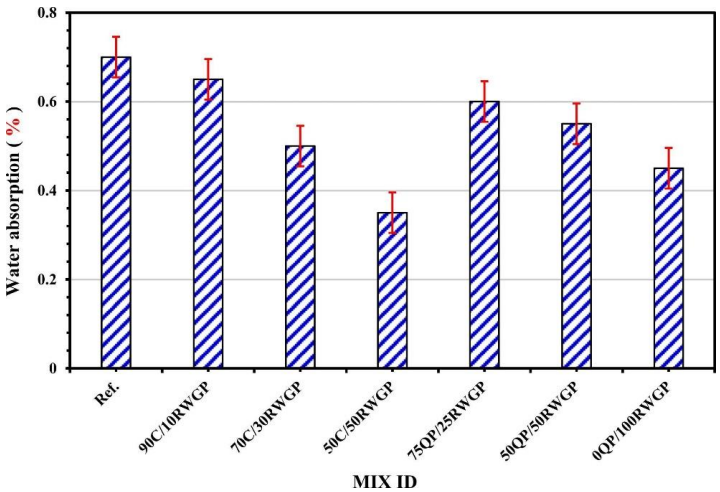

Figure 13. Water absorption of high-performance concrete containing recycled waste glass powder (RWGP) [48]

Figure 14 illustrates the correlation between the water absorption and the strength of concrete specimens with different mineral additives based on the study of Davraz et al. [52]. Upon the inclusion of 20% Seyitömer Fly Ash (SFA) in the HPC specimens, the water absorption values demonstrated a reducing trend, registering at 1.77%, 1.65%, and 1.18% for C40, C55, and C70, respectively. Similarly, HPC specimens incorporating 20% andesite waste powder (AWP) exhibited decreasing water absorption values of 1.86%, 1.65%, and 1.05% for C40, C55, and C70, respectively. The observed decrease in water absorption can be attributed to the decrease in the apparent porosity values of the concrete specimens, as shown in Figure 15. Notably, HPC specimens, particularly C50 and C70, showcased a lower water absorption ratio compared to the concrete specimen with a strength grade of C40. Such decline in water absorption and porosity correlates with the density and durability properties of the HPC specimens containing AWP, which were determined to be 20% lower than those of the control specimen. These findings collectively highlight the influence of various factors, including the inclusion of SFA and AWP, on water absorption and the resulting porosity and durability properties of HPC. Smaller pores in concrete result in lesser water absorption due to its higher resistance against water penetration [4].

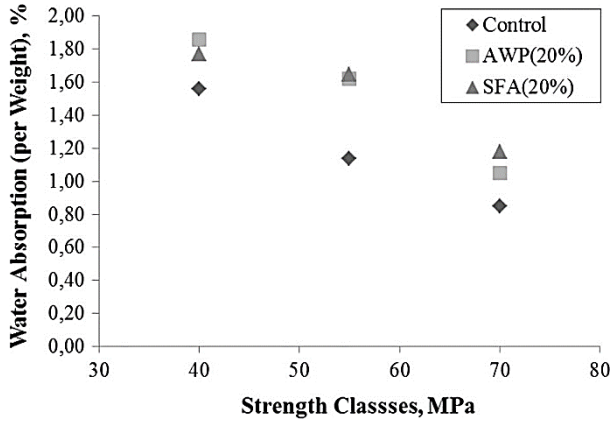

Figure 14. The correlation between the water absorption and the strength of concrete specimens with different mineral additives [52]

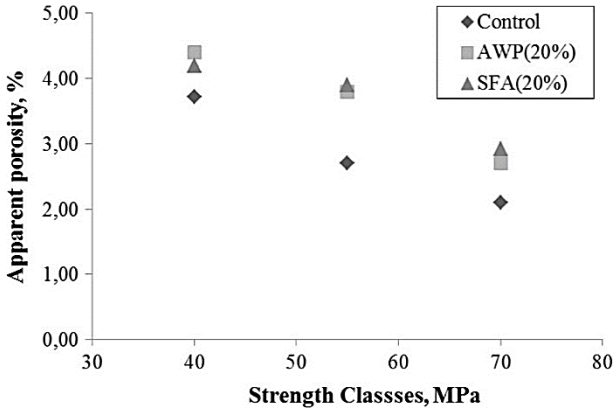

Figure 15. The correlation between the apparent porosity and the strength of concrete specimens with different mineral additives [52]

With reference to the study of Abed & Nemes [44], the results of water absorption after 90 days at atmospheric pressure for various HPC specimens are presented in Figure 16. The replacement ratio of recycled coarse aggregate (RCA) had a negligible impact on the water absorption of concrete, showing only an 18.53% increase when 50% of natural aggregate (NA) was substituted with RCA. Similar findings were reported in studies on self-compacting concrete (SCC), where water absorption in recycled aggregate concrete (RAC) remained minimal and within the recommended limits for self-consolidating high-performance concrete (SCHPC) due to the low water-to-binder (w/b) ratio. The reduced pore volume resulting from the low w/b ratio contributed to lower water absorption in the concrete. Furthermore, the choice of binder played a significant role in the water absorption behavior of concrete. Concrete incorporating waste cellular concrete powder (WCCP) exhibited higher water absorption values due to its larger particle size and higher water absorption capacity. Conversely, the inclusion of waste perlite powder (WPP) as a partial cement substitute on the 90th day of curing reduced water absorption due to its pozzolanic activity. Another noteworthy observation was that the use of unprocessed waste fly ash (UWFA) decreased the water absorption capacity of RAC. The enhanced pozzolanic activity of UWFA, combined with the water added to compensate for the water absorption capacity of RCA, contributed

to this behavior. Pozzolanic evidence of concrete was also reported by Wong et al. [5] as the strength activity index increased with an increase in curing time. The particle size distribution of UWFA played a role in filling the microcracks and pores in the RCA, resulting in decreased water absorption in the concrete.

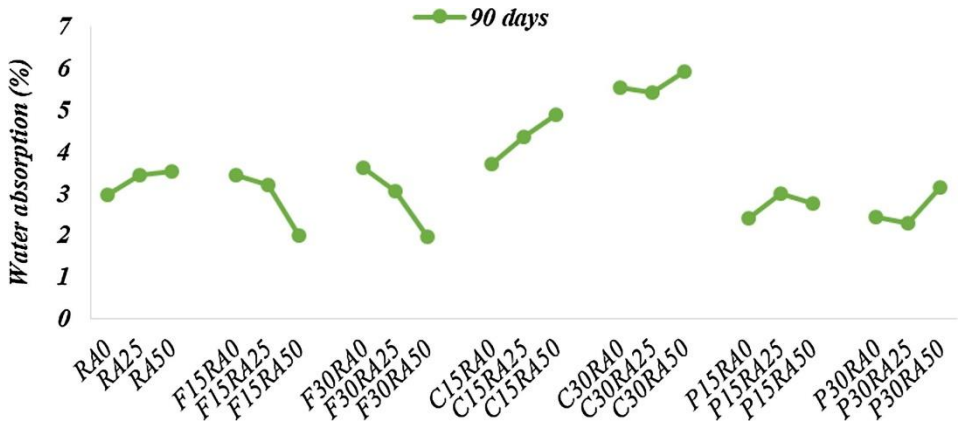

Figure 16. The results of water absorption of high-performance concrete (Note: RA is recycled aggregate, F- fly ash, C-cellular, p-perlite, at different percentages and curing) [44]

Figure 17 presents the findings on porosity and water absorption characteristics of 28-day cured HPC specimens based on the study of Liu et al. [60]. Notably, the replacement of river sand with cathode ray tube (CRT) glass demonstrated a noticeable effect on the porosity of HPC. The CRT0 concrete specimen exhibited a porosity of 4.75% at 28 days, while the CRT100 concrete specimen displayed the highest porosity, measuring at 6.88%. It is worth mentioning that the density of HPC is primarily influenced by the packing density of its particles, and as the CRT content decreases, the porosity increases accordingly. The densities of the CRT50, CRT75, and CRT100 concrete specimens were measured at 2494 kg m^{-3}, 2518 kg m^{-3}, 2563 kg m^{-3}, 2606 kg m^{-3}, and 2661 kg m^{-3}, respectively. Furthermore, the introduction of CRT glass into HPC resulted in an overall increase in density, as CRT glass possesses a higher density of 2916 kg m^{-3} compared to river sand, which has a density of 2574 kg m^{-3}.

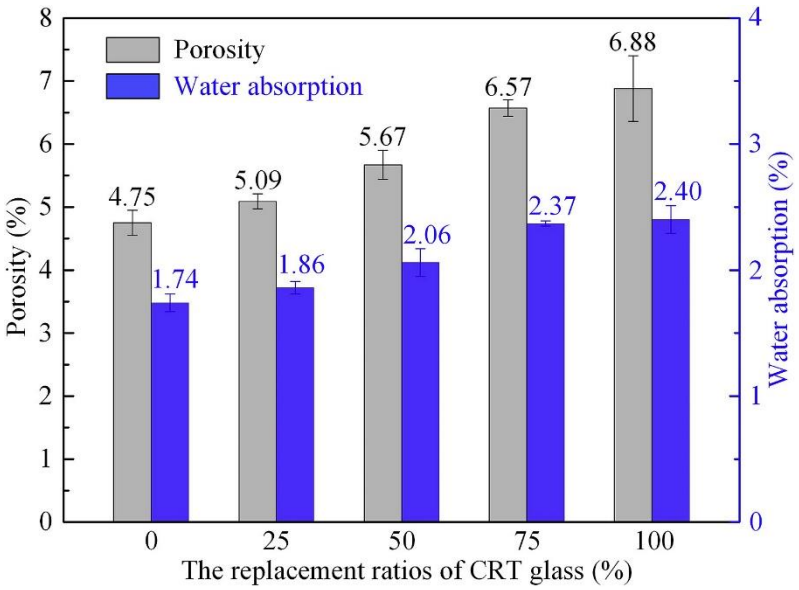

Figure 17. Effect of cathode ray tube CRT glass replacement ratios on the porosity and water absorption of high-performance concrete [60]

5. Microstructures and Chemical Compounds of High-Performance Concrete Enhanced with Recycled Waste Materials

Figure 18 exhibits the microstructural characteristics of HPC both with and without Incinerated Bottom Ash (IBA) based on the discovery of Shen et al. [45]. A distinct observation was made regarding the dense matrix of the control HPC, displaying strong bonding at the interface between the matrix and aggregates (quartz sand and IBA), indicating the absence of a significant interfacial transition zone. Such robust bonding can be attributed to the inclusion of

Supplementary Cementitious Materials (SCMs) and a low water-to-binder ratio, which facilitated the development of a denser interfacial transition zone [71]. However, the porous microstructure of IBA in the HPC was identified as a weak link, contributing to a decrease in compressive strength. It is important to note that incorporating a low amount of IBA (<25%) in the HPC led to an improvement in compressive strength, suggesting that the use of IBA in HPC can have contrasting effects on mechanical properties due to the presence of a porous structure and internal curing. The influence of the porous structure versus internal curing becomes more evident with increasing IBA dosage. With less than 25% IBA content, internal curing played a more significant role in enhancing concrete compressive strength compared to the adverse effects of the porous IBA. Conversely, incorporating more than 50% IBA content resulted in a significant reduction in concrete compressive strength due to increased porosity, which outweighed the benefits of internal curing. Consequently, HPC formulations with less than 25% IBA content achieved higher compressive strength compared to the control concrete sample.

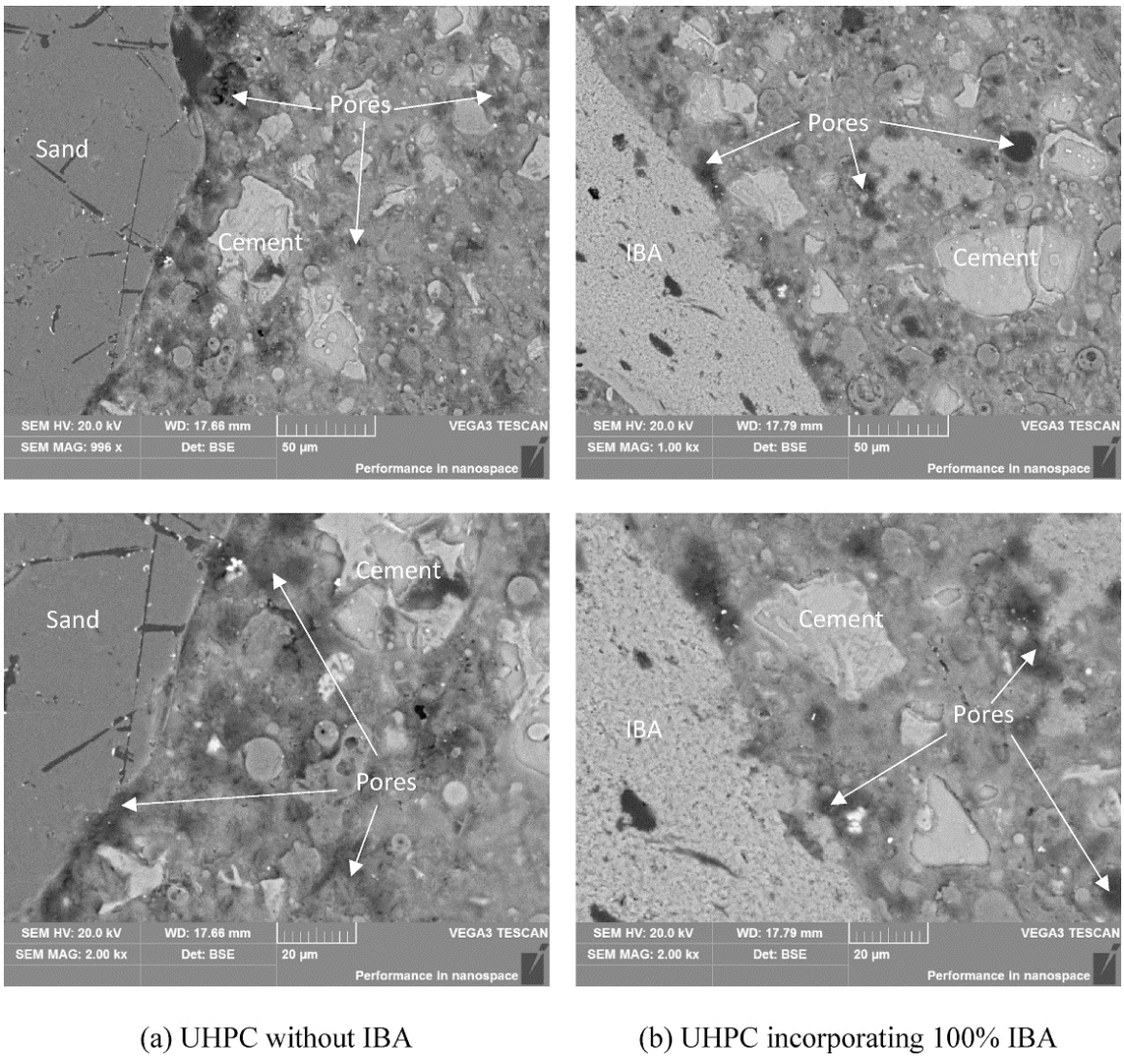

(a) UHPC without IBA (b) UHPC incorporating 100% IBA

Figure 18. Scanning Electron Microscopic images of the high-performance concrete with and without incorporating incinerated bottom ash at 28-day curing [45]

Figure 19 presents the results of Mercury Intrusion Porosimetry (MIP) test, illustrating the pore structures of the HPC samples with and without IBA. As depicted in the figure, when the IBA content increased from 0 to 100% in the HPC samples, there was an observed increase in the cumulative pore volume from 0.028 to 0.068 mL g^{-1}. Normally, concrete's compressive strength is intricately linked to its porosity and degree of hydration [72], where lower porosity typically yields higher compressive strength. Nevertheless, the study revealed a unique trend: the compressive strength initially increased when the IBA content was less than 25% and then experienced a significant decline. The inclusion of IBA in the HPC noticeably shifted the average pore size toward larger dimensions due to the presence of IBA, corroborating the microstructural observations shown in Figure 18. This coarsening effect became more pronounced with increasing IBA content.

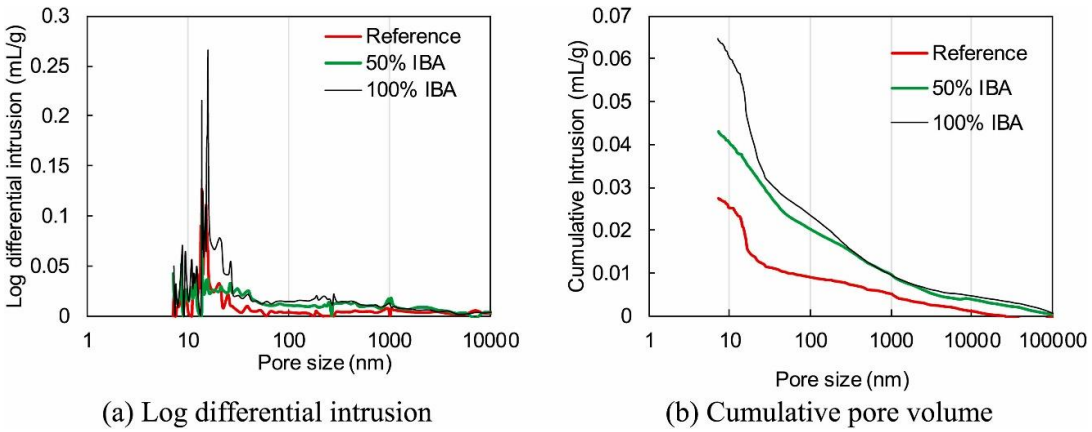

Figure 19. Pore structures of high-performance concrete with various amounts of incinerated bottom ash based on Mercury Intrusion Porosimetry (MIP) test [45]

To examine the development of hydration products in HPC samples with varying compositions of recycled waste glass powder as partial cement replacement or quartz powder replacement, scanning electron microscopic (SEM) analysis was conducted after 91 days of curing. In the 50C/50RWGP sample, 50% of the cement was replaced with recycled waste glass powder, while the 0QP/100RWGP sample fully replaced quartz powder with recycled waste glass powder. The targeted HPC properties were achieved by incorporating 200 kg m^{-3} of silica fume (SF) as a supplementary cementitious material (SCM) to provide the necessary SiO_2 content. The addition of SF resulted in a reduction of interfacial voids due to the abundant SiO_2 supplied by the reaction between SF and portlandite [$Ca(OH)_2$], a byproduct of cement hydration. Microstructural analysis, as depicted in Figure 20, revealed a highly compacted microstructure in the control concrete sample (Figure 20-a). The pozzolanic reaction of SF played a crucial role in the formation of Calcium Silicate Hydrate (C-S-H) gel, resulting in the absence of portlandite or ettringite. The interface transition zone (ITZ) in the reference mix appeared to be very thin. Moreover, the addition of recycled waste glass powder (RWGP) as a cement replacement in the 50C/50RWGP sample did not significantly impact the ITZ, as shown in Figure 20(b). SEM analysis of Figure 20-b indicated a significant formation of C-S-H after 91 days, primarily attributed to the pozzolanic reaction involving cement, SF, and RWGP. However, a decrease in C-S-H was observed in the 50C/50RWGP concrete sample compared to the control concrete, mainly due to the reduction in cement content. During the curing process of the 50C/50RWGP concrete sample, portlandite appeared to a limited extent in the cement matrix, owing to its consumption through the pozzolanic reaction between SF and RWGP, resulting in the production of C-S-H.

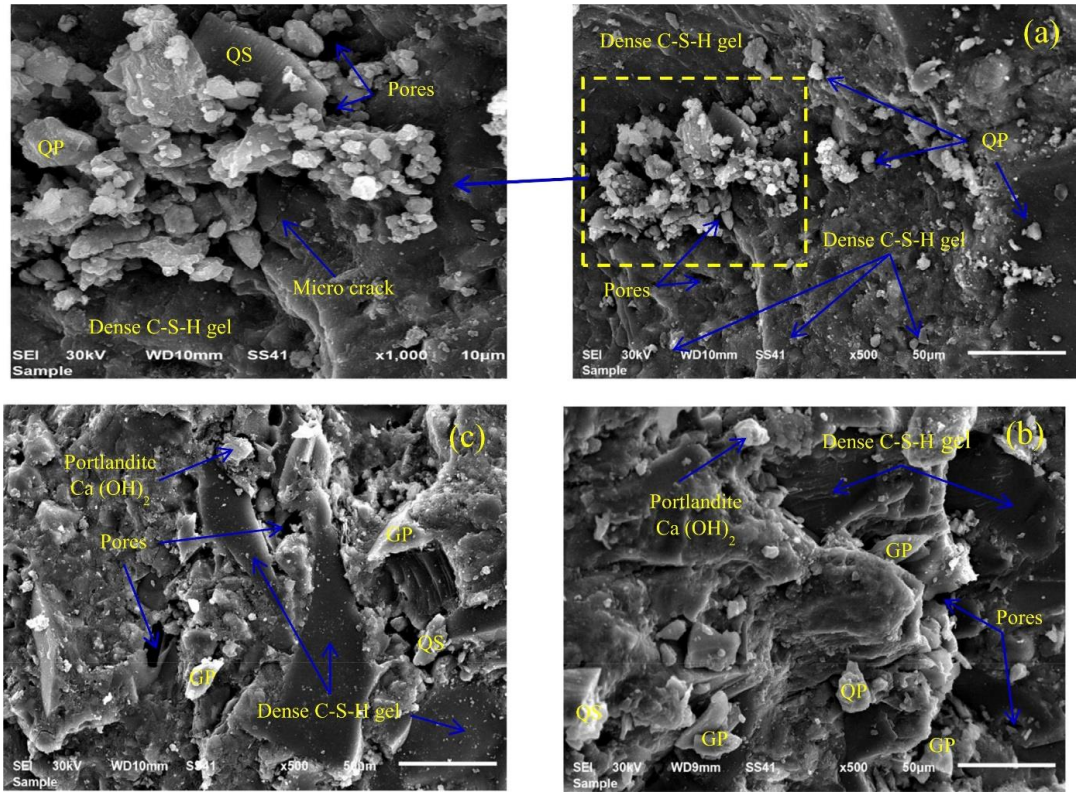

Figure 20. Scanning Electron Micrographs of recycled high-performance concrete containing waste glass powder (a) control, (b) 50C/50RWGP, and (c) 0QP/100RWGP [48]

In the 0QP/100RWGP concrete sample, the excessive use of superplasticizer resulted in the formation of numerous pores, as evident in the SEM analysis of Figure 20-c. However, extensive formation of C-S-H was observed, indicating the feasibility of incorporating RWGP in the production of HPC. SEM analysis was employed to investigate the impact of RWGP on the mechanical properties of HPC and to gain a detailed understanding of pozzolanic interactions. The HPC samples with a reduced water-to-cement ratio (w/c) contained higher quantities of glass powder (GP), quartz powder (QP), and non-reactive cement particles without the presence of visible portlandite $Ca(OH)_2$ crystals, pores, or capillary cracks. When recycled glass sand (RGS) with a particle size smaller than 125 μm interacts with portlandite [$Ca(OH)_2$], it results in the formation of hydrated calcium silicate (C-S-H) with a relatively low Ca/Si ratio. The amorphous portlandite $Ca(OH)_2$ reacts with dissolved silica, inhibiting the formation of expansive Alkali-Silica Reaction (ASR) gels in the HPC

Figure 21 demonstrates the comparison of particle surfaces, highlighting a noticeable reduction in surface roughness of Cathode Ray Tube (CRT) glass particles in contrast to river sand. This decrease in surface roughness played a pivotal role in influencing the properties of HPC when CRT was employed as a substitute for sand. The flowability of HPC exhibited a consistent augmentation as the CRT glass replacement ratio progressed from 0 to 75%. However, when reaching 100% replacement, the mixture exclusively comprised coarse aggregates ranging from 0.6 to 1.18 mm, resulting in a substantial decrease in particle packing density. While the reduction in surface roughness was evident, it was primarily the decline in particle packing density that exerted the most significant influence on flowability. Consequently, the overall flowability diminished as the replacement ratio of CRT glass increased from 75 to 100%.

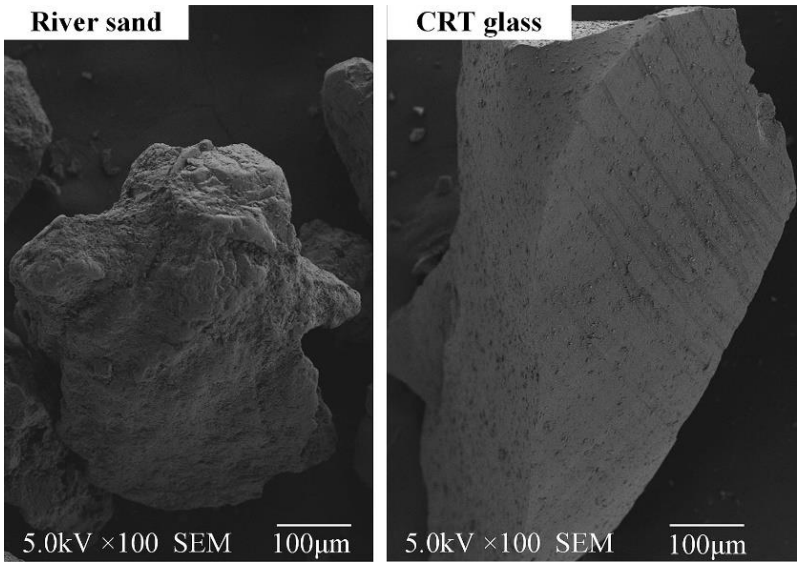

Figure 21. Scanning Electron Microscopic images of river sand and CRT glass [60]

Figure 22 illustrates the XRD patterns of HPC specimens with different CRT proportions at 28 days. The investigation unveiled several primary phases in the HPC samples, including $Ca(OH)_2$ (detected at 18.1°), ettringite (detected at 9.6°), crystallized C-S-H (detected at 29.6°), and unhydrated cement clinker (C_2S/ C_3S, detected at 32.3° and 32.8°). Peaks observed at 26.1°, 26.8°, 39.6°, 42.5°, 50.3°, and 60.0° indicated the presence of SiO_2. The strength of the peaks in the XRD pattern is directly correlated with the relative quantity of each primary phase present in the HPC sample [73, 74]. Notably, the strength of the SiO_2 peaks in the control (CRT0) sample exceeded that of the other four HPC samples, suggesting a decrease in the proportionate quantity of SiO_2 upon the inclusion of CRT glass. This decline can be attributed to the lower SiO_2 composition in CRT glass (55.6 wt%) compared to river sand (67 wt%). Significant contrasts in peak intensity were observed between C_2S/ C_3S and crystallized C-S-H when comparing the XRD pattern of CRT0 to the XRD patterns of CRT25 (25% replacement), CRT50 (50% replacement), CRT75 (75% replacement), and CRT100 (100% replacement). The peak intensity of C_2S/ C_3S became more pronounced, while the peak intensity of crystallized C-S-H decreased in the XRD patterns of CRT25, CRT50, CRT75, and CRT100. The addition of CRT glass resulted in an increase in the intensity of the C_2S/ C_3S peak, indicating a higher level of unhydrated cement. Conversely, the presence of CRT glass led to a decrease in the peak intensity of crystallized C-S-H, suggesting its hindrance in C-S-H formation. This hindrance can be attributed to the leached lead from untreated CRT glass forming a coating on the surface of cement particles and impeding their interaction with water. As a result, the hydration process is hindered, leading to a slower formation of C-S-H [75, 76]. The reduced amount of C-S-H due to the presence of CRT glass is one of the factors contributing to the reduced mechanical strength of HPC. A higher quantity of C-S-H is known to contribute to a more compact and tightly packed microstructure of HPC [77].

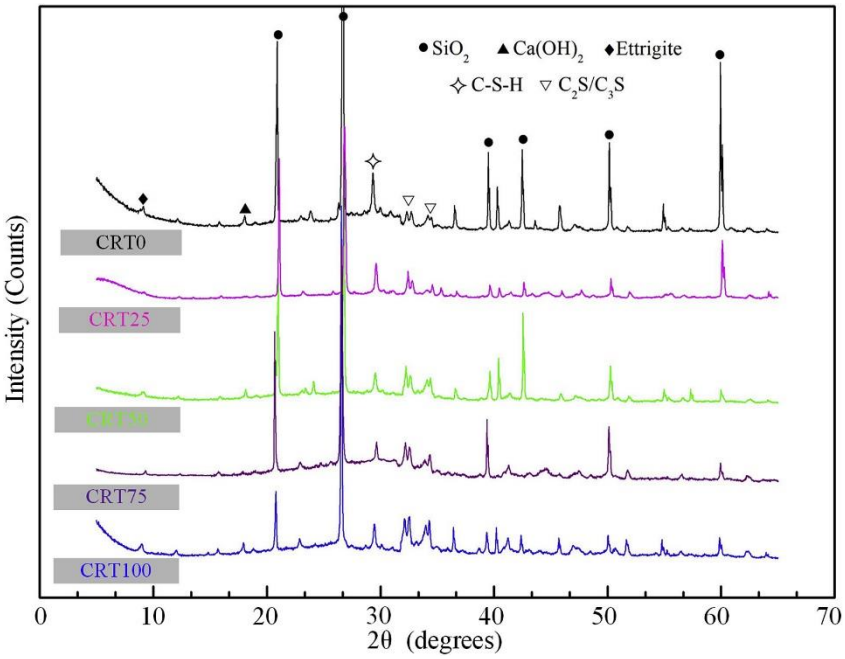

Figure 22. X-ray diffraction patterns for high-performance concrete samples with different replacement ratios of cathode ray tube (CRT) glass at 28 days [60]

Images in Figure 23 showcase the microstructures for the HPC samples with a fine aggregate-to-ceramic waste aggregate ratio of 1:1, 20% cement replacement by silica fume (SF20), and 20% cement replacement by metakaolin (MK20). The provided visuals offered valuable observations regarding the influence of replacing 20% of SF and MK (Metakaolin) on the microstructure. A clear observation emerged, revealing that SF20 and MK20 exhibited reduced porosity when compared to the control sample. This decline in porosity can be attributed to the higher proportion of SiO_2 present in SF and MK materials compared to cement. The reaction between SF and MK materials and the byproduct of cement hydration, $Ca(OH)_2$, played a significant role in decreasing the presence of voids, compensating for the decrease in C-S-H. The distribution of C-S-H gel was found to be extensive throughout the HPC. However, contrasting observations were made regarding the control, SF20, and MK20 HPC specimens after 7 days, revealing evident gaps and a less compact microstructure within the cement paste. Various products resulting from hydration were detected, such as fibrous and honeycomb-shaped C-S-H formations, elongated and needle-like ettringite (AFt), and inadequately hydrated calcium hydroxide plates. These discoveries indicated inadequate hydration reactions in the concrete within the 7-day timeframe. Consequently, subsequent hydration reactions ensued, effectively occupying the void spaces between aggregates and cement paste, with C-S-H exhibiting distinct crystalline characteristics and the formation of second-generation compounds [78].

Figure 24 presents the SEM and EDX analysis of the morphology of HPC incorporating different types of Supplementary Cementitious Materials (SCMs). All the mixtures contain a fixed amount of silica fume and another type of SCMs in varying amounts, replacing cement, to form a ternary binder. The microstructure of HPC varied depending on the SCMs incorporated. The GGBS30 mixture (30% cement replacement by GGBS) exhibited a less compact and denser microstructure compared to the control mixture (M0), as shown in Figure 24(a) and (b). The presence of unreacted particles and interfacial fissures in the control mixture indicated microstructural brittleness and incomplete hydration. The GGBS30 samples showed the largest pore size among all the HPC mixes investigated (Figure 24(b)). When GGBS was introduced, it had a negative impact on the connection point between the binder and aggregate, leading to a less compact microstructure and the existence of unreacted particles. Likewise, the FA20 blend (with 20% of cement replaced by fly ash) displayed comparable outcomes, with fly ash adversely influencing the microstructure of the high-performance concrete, as depicted in Figure 24(c). Surprisingly, the FA20 concoction displayed a microstructure characterized by reduced porosity, owing to the greater abundance of SiO_2 contributed by fly ash in contrast to cement.

Furthermore, the presence of fewer interfacial voids and the interaction between silica fume, fly ash, and portlandite acted as a compensatory mechanism for the absence of C-S-H. The SEM images provided visual confirmation of the uniformly dispersed C-S-H gel within the structure of the HPC sample. Furthermore, through the utilization of SEM imaging, it was revealed that the introduction of 15% metakaolin as a cement substitute resulted in a remarkable enhancement of the microstructure within the MK15 blend, as exemplified in Figure 24(d). These

discoveries closely align with prior research [79, 80], affirming that the integration of supplementary phases contributed to an overall improvement in the microstructure. The effects of incorporating SCMs on the composition of HPC were further elucidated through EDX analysis, as depicted in Figure 24(e-h). In the control (M0) and MK15 samples, the primary ingredients of cementitious products, such as Ca, Si, and O, exhibited significant peaks. This signifies their hydraulic reactivity and their capacity to interact with $Ca(OH)_2$, leading to the generation of supplementary C-S-H gel. Furthermore, the introduction of SCMs yielded noticeable alterations in the elemental composition, as observed through EDX analysis. The incorporation of MK exhibited elevated levels of Si, Fe, and Ca in comparison to the control concrete sample. Conversely, the inclusion of FA and GGBS resulted in a reduction in the concentration of Si and Fe elements.

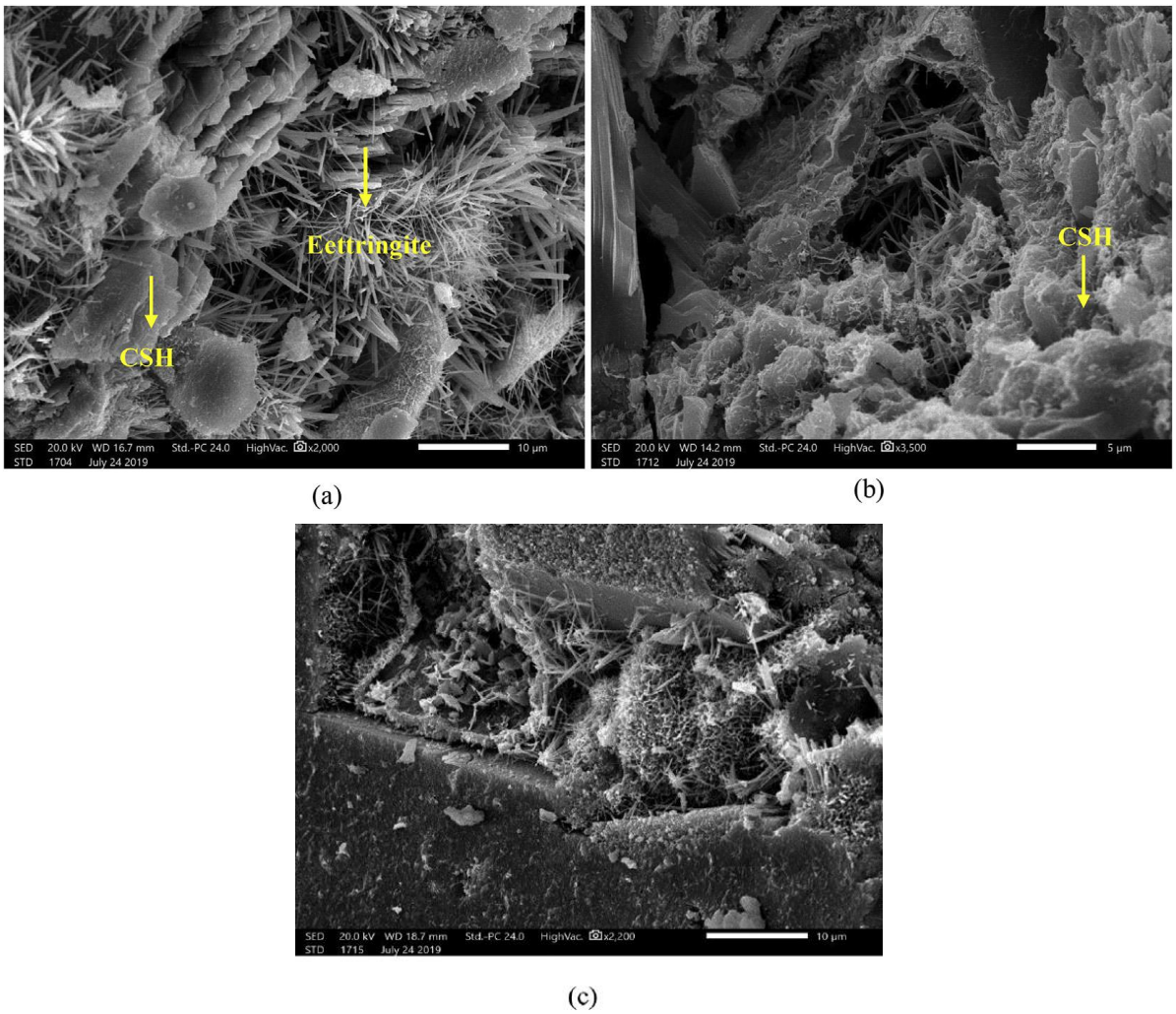

Figure 23. Scanning Electron Microscopic images at 7 days (a) HPC with fine aggregate-to-ceramic waste aggregates ratio at 1:1, (b) HPC with 20% cement replacement by silica fume and (c) HPC with 20% cement replacement by metakaolin [49]

At the 28-day mark, Figure 25 displays the XRD patterns of the HPC samples that include various types of supplementary cementitious materials (SCMs). It should be noted that the intensity of diffraction peaks in the X-ray scan rate can be influenced, as evident in relevant literature [81, 82]. The intensity of the peaks observed in the XRD spectra directly corresponds to the quantity of hydration products present. Peaks within the range of 20° to 44° were detected in all HPC samples. Interestingly, the intensity of the peak associated with SiO_2 in the HPC samples containing both FA and MK was comparable to that of the control concrete sample. Figure 25(b) illustrates that GGBS led to varying degrees of increased peaks related to SiO_2 and other hydration products, which aligns with similar observations reported in previous studies [82, 83]. The primary phases identified in the control concrete sample include portlandite and ettringite. It was observed that the incorporation of different types of SCMs reduced the content of ettringite. Furthermore, peaks related to non-hydrated cement particles such as C_3S, C_2S, and C_4AF were still present in the cement-rich HPC samples. The content of non-hydrated cement particles varied depending on the incorporation of different SCMs, corroborating findings from previous studies examining the effects of SCMs on HPC characteristics [84].

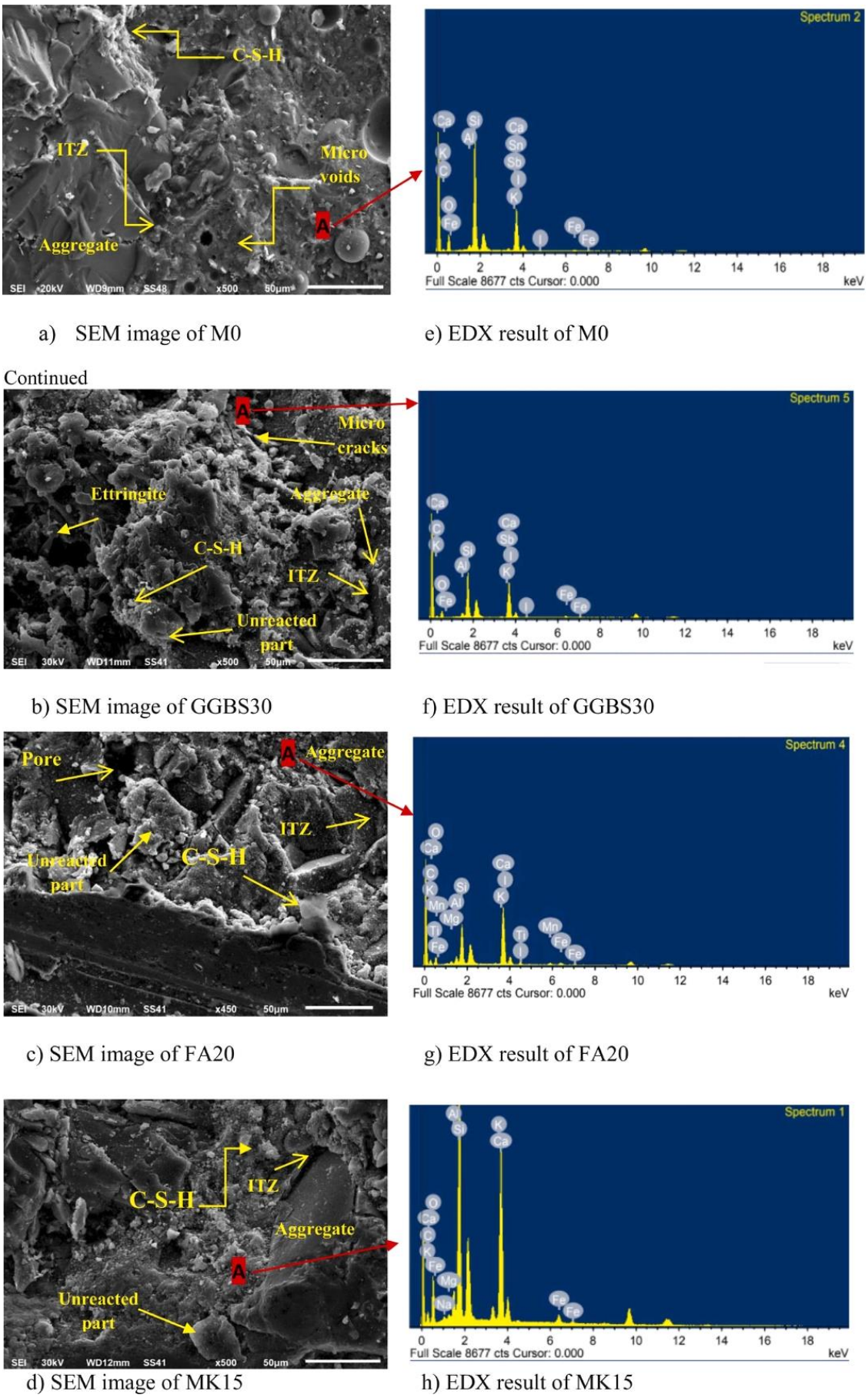

Figure 24. Scanning Electron Microscopic and Energy Dispersive X-ray of high-performance concrete samples incorporating different types of Supplementary Cementitious Materials (a) reference mix, (b) 30% cement replacement by GGBS, (c) 20% cement replacement by fly ash and (d) 15% cement replacement by metakaolin [58].

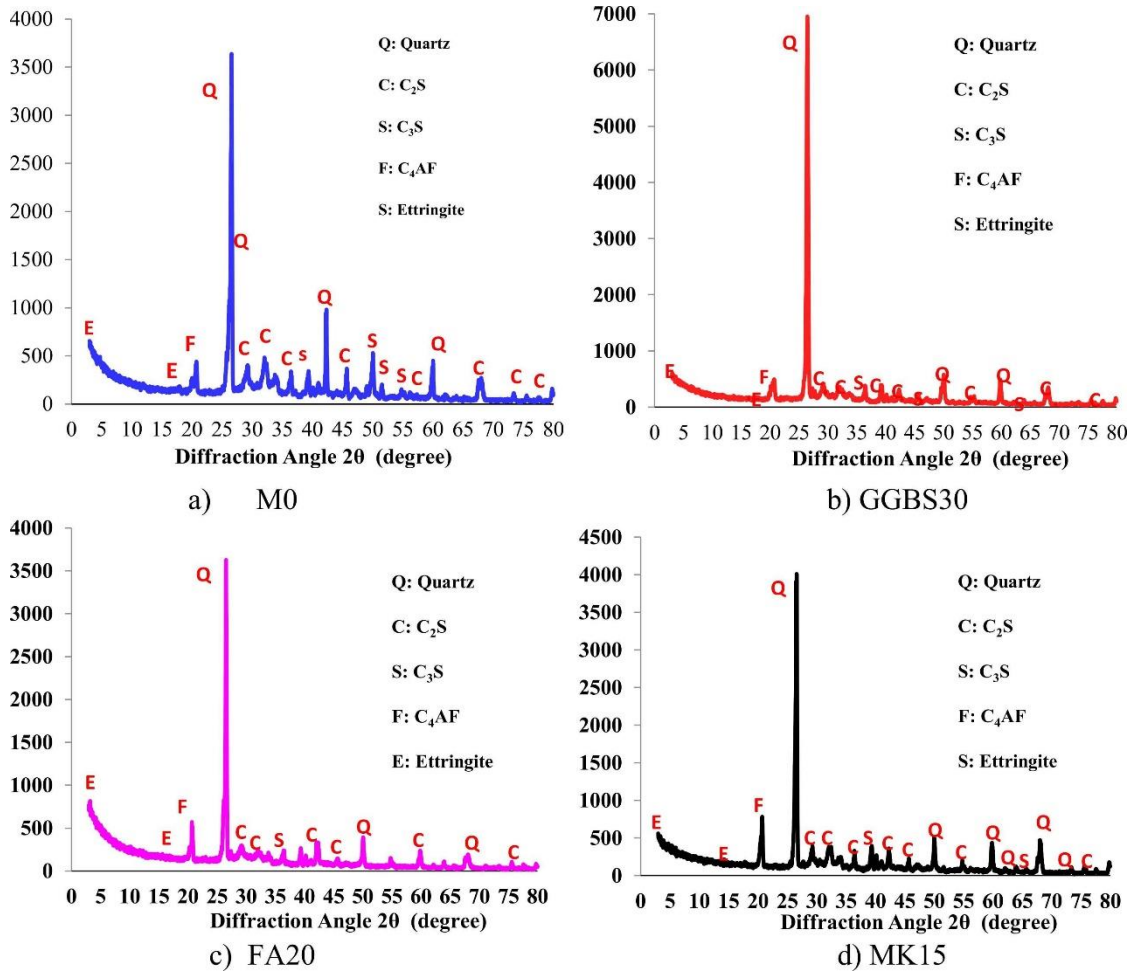

Figure 25. X-ray diffraction pattern of high-performance concrete samples tested at 28 days (a) control sample (M0), (b) 30% cement replacement by GGBS (GGBS30), (c) 20% cement replacement by fly ash (FA20) and (d) 15% cement replacement by metakaolin (MK15) [58].

6. Conclusions

This paper presents a critical review of the characteristics of HPC produced using various types of recycled waste materials to partially replace cement, sand, and coarse aggregate. By incorporating waste materials, the construction industry can make use of sustainable alternatives and reduce its reliance on natural resources. The previous findings are summarized below:

- Previous studies have explored the potential of various waste materials, such as porous ceramic coarse aggregate, recycled coarse aggregate, waste incineration bottom ash, copper slag, calcined marine clay, glass powder, cathode ray tube (CRT) glass, and foundry slag, as replacements for traditional aggregates. The optimal proportion of each waste material varied depending on factors such as surface texture, microstructures, size distribution, and chemical compositions. While both porous ceramic coarse aggregate and incineration bottom ash can provide internal curing to high-performance concrete (HPC), their incorporation in large quantities may lead to a reduction in strength due to their weak porous microstructures. To maintain the performance of HPC without negative effects, it was reported that incinerated bottom ash can be incorporated at levels below 25%, while the addition of 40% porous ceramic coarse aggregate effectively reduces internal stress without causing shrinkage.
- Furthermore, incorporating 40% copper slag enhances the performance of the HPC mix, and the use of recycled coarse aggregate (RCA) as a replacement can reach up to 50% in self-compacting high-performance concrete without significant impacts on its durability properties. Foundry slag is feasible within the range of 10% to 45% incorporation. The inclusion of glass powder in HPC with straight steel fibers demonstrates positive results, as it increases shear resistance at the interface between the fibers and the concrete matrix, thereby improving frictional properties. On the other hand, replacing QP with low-grade marine clay leads to a 10% decrease in strength, while cathode ray tube glass negatively affects compressive and flexural strength due to its smooth surface texture.
- Extensive research has been conducted on various materials that can partially replace cement, including fly ash, recycled waste glass powder, silica fume, rice husk ash, andesite, waste perlite powder, metakaolin, basalt powder,

and alccofine. Among these materials, fly ash, silica fume, and metakaolin have received the most attention due to their widespread availability. The use of fly ash as a substitute for cement, up to a 15% replacement, has shown remarkable durability. Likewise, the substitution of cement with either silica fume or metakaolin has demonstrated encouraging outcomes in augmenting the physical and mechanical characteristics of top-quality concrete. Notable advancements have been proven with the inclusion of 15% metakaolin, resulting in heightened compressive, flexural, and splitting tensile strengths along with fortified resilience against chloride permeability. Furthermore, a combination of 10% rice husk ash and 10% silica fume in the concrete mixture has demonstrated exceptional compressive strength when compared to the standard concrete specimen.

- Introducing 10% recycled waste glass powder (RWGP) as a replacement for cement has been found to significantly enhance the interfacial transition zone. Furthermore, an optimal cement replacement for HPC of 10% has been identified for andesite waste powder, while it was determined to be 15% for alccofine. It is worth noting that the internal curing provided by nano waste glass, nano rice husk ash, nanometakaolin, and nanosilica has resulted in improved concrete compressive strength.

7. Declarations

7.1. Author Contributions

Conceptualization, A.M.D.A.J.; validation, L.S.W.; formal analysis, A.M.D.A.J. and L.S.W.; investigation, A.M.D.A.J.; writing—original draft preparation, A.M.D.A.J. and L.S.W.; writing—review and editing, S.Y.K., A.W.A.Z, and M.A.K.M.; supervision, L.S.W., S.Y.K., and A.W.A.Z; funding acquisition, A.M.D.A.J. All authors have read and agreed to the published version of the manuscript.

7.2. Data Availability Statement

Data sharing is not applicable to this article.

7.3. Funding

The Ministry of Higher Education Malaysia, through the Fundamental Research Grant Scheme (FRGS), grant number FRGS/1/2022/TK01/UNITEN/02/1, has generously provided funding for the authors' research work relevant to this review article.

7.4. Conflicts of Interest

The authors declare no conflict of interest.

8. References

[1] Esquinas, A. R., Ledesma, E. F., Otero, R., Jiménez, J. R., & Fernández, J. M. (2018). Mechanical behaviour of self-compacting concrete made with non-conforming fly ash from coal-fired power plants. Construction and Building Materials, 182, 385–398. doi:10.1016/j.conbuildmat.2018.06.094.

[2] Aslani, F., Ma, G., Yim Wan, D. L., & Muselin, G. (2018). Development of high-performance self-compacting concrete using waste recycled concrete aggregates and rubber granules. Journal of Cleaner Production, 182, 553–566. doi:10.1016/j.jclepro.2018.02.074.

[3] de Brito, J., & Kurda, R. (2021). The past and future of sustainable concrete: A critical review and new strategies on cement-based materials. Journal of Cleaner Production, 281, 123558. doi:10.1016/j.jclepro.2020.123558.

[4] Wong, L. S., Oweida, A. F. M., Kong, S. Y., Iqbal, D. M., & Regunathan, P. (2020). The surface coating mechanism of polluted concrete by Candida ethanolica induced calcium carbonate mineralization. Construction and Building Materials, 257, 119482. doi:10.1016/j.conbuildmat.2020.119482.

[5] Wong, L. S., Chandran, S. N., Rajasekar, R. R., & Kong, S. Y. (2022). Pozzolanic characterization of waste newspaper ash as a supplementary cementing material of concrete cylinders. Case Studies in Construction Materials, 17, 1342. doi:10.1016/j.cscm.2022.e01342.

[6] Şanal, İ. (2018). Discussion on the effectiveness of cement replacement for carbon dioxide (CO2) emission reduction in concrete. Greenhouse Gases: Science and Technology, 8(2), 366–378. doi:10.1002/ghg.1748.

[7] Zidol, A., Tognonvi, M. T., & Tagnit-Hamou, A. (2021). Concrete incorporating glass powder in aggressive environments. ACI Materials Journal, 118(2), 43–52. doi:10.14359/51729326.

[8] Hamada, H. M., Skariah Thomas, B., Tayeh, B., Yahaya, F. M., Muthusamy, K., & Yang, J. (2020). Use of oil palm shell as an aggregate in cement concrete: A review. Construction and Building Materials, 265, 120357. doi:10.1016/j.conbuildmat.2020.120357.

[9] Hamada, H. M., Tayeh, B. A., Al-Attar, A., Yahaya, F. M., Muthusamy, K., & Humada, A. M. (2020). The present state of the use of eggshell powder in concrete: A review. Journal of Building Engineering, 32, 101583. doi:10.1016/j.jobe.2020.101583.

[10] Zhang, W., Liu, X., Huang, Y., & Tong, M. N. (2022). Reliability-based analysis of the flexural strength of concrete beams reinforced with hybrid BFRP and steel rebars. Archives of Civil and Mechanical Engineering, 22(4), 1–20. doi:10.1007/s43452-022-00493-7.

[11] zhang, W., & Huang, Y. (2022). Three-dimensional numerical investigation of mixed-mode debonding of FRP-concrete interface using a cohesive zone model. Construction and Building Materials, 350, 128818. doi:10.1016/j.conbuildmat.2022.128818.

[12] Huang, H., Huang, M., Zhang, W., Pospisil, S., & Wu, T. (2020). Experimental Investigation on Rehabilitation of Corroded RC Columns with BSP and HPFL under Combined Loadings. Journal of Structural Engineering, 146(8), 4020157. doi:10.1061/(asce)st.1943-541x.0002725.

[13] Hu, Z., Shi, T., Cen, M., Wang, J., Zhao, X., Zeng, C., Zhou, Y., Fan, Y., Liu, Y., & Zhao, Z. (2022). Research progress on lunar and Martian concrete. Construction and Building Materials, 343, 128117. doi:10.1016/j.conbuildmat.2022.128117.

[14] Yuan, J., Lei, D., Shan, Y., Tong, H., Fang, X., & Zhao, J. (2022). Direct Shear Creep Characteristics of Sand Treated with Microbial-Induced Calcite Precipitation. International Journal of Civil Engineering, 20(7), 763–777. doi:10.1007/s40999-021-00696-8.

[15] Lan, Y., Zheng, B., Shi, T., Ma, C., Liu, Y., & Zhao, Z. (2022). Crack resistance properties of carbon nanotube-modified concrete. Magazine of Concrete Research, 74(22), 1165–1175. doi:10.1680/jmacr.21.00227.

[16] Shan, Y., Zhao, J., Tong, H., Yuan, J., Lei, D., & Li, Y. (2022). Effects of activated carbon on liquefaction resistance of calcareous sand treated with microbially induced calcium carbonate precipitation. Soil Dynamics and Earthquake Engineering, 161, 107419. doi:10.1016/j.soildyn.2022.107419.

[17] Shi, T., Liu, Y., Zhang, Y., Lan, Y., Zhao, Q., Zhao, Y., & Wang, H. (2022). Calcined Attapulgite Clay as Supplementary Cementing Material: Thermal Treatment, Hydration Activity and Mechanical Properties. International Journal of Concrete Structures and Materials, 16(1), 1–10. doi:10.1186/s40069-022-00499-8.

[18] Zhang, C., & Ali, A. (2021). The advancement of seismic isolation and energy dissipation mechanisms based on friction. Soil Dynamics and Earthquake Engineering, 146, 106746. doi:10.1016/j.soildyn.2021.106746.

[19] Gong, P., Wang, D., Zhang, C., Wang, Y., Jamili-Shirvan, Z., Yao, K., & Wang, X. (2022). Corrosion behavior of TiZrHfBeCu(Ni) high-entropy bulk metallic glasses in 3.5 wt. % NaCl. NPJ Materials Degradation, 6(1), 1–14. doi:10.1038/s41529-022-00287-5.

[20] Sharma, D., Sharma, S., & Goyal, A. (2016). Utilization of waste foundry slag and alccofine for developing high strength concrete. International Journal of Electrochemical Science, 11(4), 3190–3205. doi:10.20964/110403190.

[21] ACI 363R-92. (1992). Report on High-Strength Concrete. Reported by ACI Committee 363, American Concrete Institute, Detroit, United States.

[22] Meyer, C. (2009). The greening of the concrete industry. Cement and Concrete Composites, 31(8), 601–605. doi:10.1016/j.cemconcomp.2008.12.010.

[23] Allwood, J. M., Cullen, J. M., & Milford, R. L. (2010). Options for achieving a 50% cut in industrial carbon emissions by 2050. Environmental Science and Technology, 44(6), 1888–1894. doi:10.1021/es902909k.

[24] Ali, M. B., Saidur, R., & Hossain, M. S. (2011). A review on emission analysis in cement industries. Renewable and Sustainable Energy Reviews, 15(5), 2252–2261. doi:10.1016/j.rser.2011.02.014.

[25] El Mir, A., & Nehme, S. G. (2017). Utilization of industrial waste perlite powder in self-compacting concrete. Journal of Cleaner Production, 156, 507–517. doi:10.1016/j.jclepro.2017.04.103.

[26] Reddy, C. S., Ratnasai, K. V., Rathish Kumar, P., & Rajesh Kumar, P. (2013). Recycled aggregate based self-compacting concrete (RASCC) for structural applications. Technical Paper Presented in RN Raikar Memorial International Conference; India Chapter of American Concrete Institute (ICACI), December, 20-21, 2013, Mumbai, India.

[27] Zhang, P., Wan, J., Wang, K., & Li, Q. (2017). Influence of nano-SiO2 on properties of fresh and hardened high performance concrete: A state-of-the-art review. Construction and Building Materials, 148, 648–658. doi:10.1016/j.conbuildmat.2017.05.059.

[28] Randl, N., Steiner, T., Ofner, S., Baumgartner, E., & Mészöly, T. (2014). Development of UHPC mixtures from an ecological point of view. Construction and Building Materials, 67(PART C), 373–378. doi:10.1016/j.conbuildmat.2013.12.102.

[29] Wee, T. H., Matsunaga, Y., Watanabe, Y., & Sakai, E. (1995). Microstructure and strength properties of high strength concretes containing various mineral admixtures. Cement and Concrete Research, 25(4), 715–720. doi:10.1016/0008-8846(95)00061-G.

[30] Baker, M. A., & Ismael, N. S. (2008). Using of Waste Materials for Production of High Performance Concrete. Journal of Techniques, 21(4).

[31] Yuliarti, K., Susilorini, R., & Aboubakr, A. (2015). Properties of Ultra High Performance Concrete. Proceedings of International Conference on Concrete and Infrastructure 2015, 28-30 October, 2015, Semarang, Indonesia.

[32] Meyer, C., Vishwakarma, V., Xie, X., Gou, Z., & Lawrence, T. (2002). Concrete for the new century. Association of New York City Concrete Producers Spring/Summer, New York, United States.

[33] El-Abbasy, A. A. (2022). Production, behaviour and mechanical properties of ultra-high-performance fiber concrete – A comprehensive review. Case Studies in Construction Materials, 17, 1637. doi:10.1016/j.cscm.2022.e01637.

[34] Gong, J., Ma, Y., Fu, J., Hu, J., Ouyang, X., Zhang, Z., & Wang, H. (2022). Utilization of fibers in ultra-high performance concrete: A review. Composites Part B: Engineering, 241, 109995. doi:10.1016/j.compositesb.2022.109995.

[35] Wen, C., Zhang, P., Wang, J., & Hu, S. (2022). Influence of fibers on the mechanical properties and durability of ultra-high-performance concrete: A review. Journal of Building Engineering, 52, 104370. doi:10.1016/j.jobe.2022.104370.

[36] Hamada, H., Alattar, A., Tayeh, B., Yahaya, F., & Thomas, B. (2022). Effect of recycled waste glass on the properties of high-performance concrete: A critical review. Case Studies in Construction Materials, 17, 1149. doi:10.1016/j.cscm.2022.e01149.

[37] Ahmed, K. S., & Rana, L. R. (2023). Fresh and hardened properties of concrete containing recycled waste glass: A review. Journal of Building Engineering, 70, 1063127. doi:10.1016/j.jobe.2023.106327.

[38] Tayeh, B. A., Saffar, D. M. A., & Alyousef, R. (2020). The Utilization of Recycled Aggregate in High Performance Concrete: A Review. Journal of Materials Research and Technology, 9(4), 8469–8481. doi:10.1016/j.jmrt.2020.05.126.

[39] Salas_Montoya, A., Chung, C. W., & Mira_Rada, B. E. (2023). Interaction effect of recycled aggregate type, moisture state, and mixing process on the properties of high-performance concretes. Case Studies in Construction Materials, 18, 2208. doi:10.1016/j.cscm.2023.e02208.

[40] Alyaseen, A., Poddar, A., Alahmad, H., Kumar, N., & Sihag, P. (2023). High-performance self-compacting concrete with recycled coarse aggregate: comprehensive systematic review on mix design parameters. Journal of Structural Integrity and Maintenance, 8(3), 161–178. doi:10.1080/24705314.2023.2211850.

[41] Hamada, H., Abed, F., Alattar, A., Yahaya, F., Tayeh, B., & Aisheh, Y. I. A. (2023). Influence of palm oil fuel ash on the high strength and ultra-high performance concrete: A comprehensive review. Engineering Science and Technology, an International Journal, 45, 101492. doi:10.1016/j.jestch.2023.101492.

[42] Tran, N. P., Nguyen, T. N., Ngo, T. D., Le, P. K., & Le, T. A. (2022). Strategic progress in foam stabilisation towards high-performance foam concrete for building sustainability: A state-of-the-art review. Journal of Cleaner Production, 375, 133939. doi:10.1016/j.jclepro.2022.133939.

[43] Su, W., Liu, J., Liu, L., Chen, Z., & Shi, C. (2023). Progresses of high-performance coral aggregate concrete (HPCAC): A review. Cement and Concrete Composites, 140, 105059. doi:10.1016/j.cemconcomp.2023.105059.

[44] Abed, M., & Nemes, R. (2019). Long-term durability of self-compacting high-performance concrete produced with waste materials. Construction and Building Materials, 212, 350–361. doi:10.1016/j.conbuildmat.2019.04.004.

[45] Shen, P., Zheng, H., Xuan, D., Lu, J. X., & Poon, C. S. (2020). Feasible use of municipal solid waste incineration bottom ash in ultra-high performance concrete. Cement and Concrete Composites, 114, 103814. doi:10.1016/j.cemconcomp.2020.103814.

[46] Malkhare, S. S., & Pujari, A. B. (2018). To Study the Performance of Copper Slag As Partial or Fully Replacement to Fine Aggregates in Concrete. International Journal of Research & Review, 5(5), 102.

[47] Gonzalez-Corominas, A., & Etxeberria, M. (2014). Properties of high performance concrete made with recycled fine ceramic and coarse mixed aggregates. Construction and Building Materials, 68, 618–626. doi:10.1016/j.conbuildmat.2014.07.016.

[48] Tahwia, A. M., Essam, A., Tayeh, B. A., & Elrahman, M. A. (2022). Enhancing sustainability of ultra-high performance concrete utilizing high-volume waste glass powder. Case Studies in Construction Materials, 17, 1648. doi:10.1016/j.cscm.2022.e01648.

[49] Amin, M., Tayeh, B. A., & Agwa, I. S. (2020). Effect of using mineral admixtures and ceramic wastes as coarse aggregates on properties of ultrahigh-performance concrete. Journal of Cleaner Production, 273, 123073. doi:10.1016/j.jclepro.2020.123073.

[50] Van Tuan, N., Ye, G., Van Breugel, K., Fraaij, A. L. A., & Bui, D. D. (2011). The study of using rice husk ash to produce ultra-high performance concrete. Construction and Building Materials, 25(4), 2030–2035. doi:10.1016/j.conbuildmat.2010.11.046.

[51] Dixit, A., Verma, A., & Pang, S. D. (2021). Dual waste utilization in ultra-high performance concrete using biochar and marine clay. Cement and Concrete Composites, 120, 104049. doi:10.1016/j.cemconcomp.2021.104049.

[52] Davraz, M., Ceylan, H., Topçu, İ. B., & Uygunoğlu, T. (2018). Pozzolanic effect of andesite waste powder on mechanical properties of high strength concrete. Construction and Building Materials, 165, 494–503. doi:10.1016/j.conbuildmat.2018.01.043.

[53] Xu, K., Huang, W., Zhang, L., Fu, S., Chen, M., Ding, S., & Han, B. (2021). Mechanical properties of low-carbon ultrahigh-performance concrete with ceramic tile waste powder. Construction and Building Materials, 287, 123036. doi:10.1016/j.conbuildmat.2021.123036.

[54] AlKhatib, A., Maslehuddin, M., & Al-Dulaijan, S. U. (2020). Development of high performance concrete using industrial waste materials and nano-silica. Journal of Materials Research and Technology, 9(3), 6696–6711. doi:10.1016/j.jmrt.2020.04.067.

[55] Wang, J., Mu, M., & Liu, Y. (2018). Recycled cement. Construction and Building Materials, 190, 1124–1132. doi:10.1016/j.conbuildmat.2018.09.181.

[56] Li, Y., Zeng, X., Zhou, J., Shi, Y., Umar, H. A., Long, G., & Xie, Y. (2021). Development of an eco-friendly ultra-high performance concrete based on waste basalt powder for Sichuan-Tibet Railway. Journal of Cleaner Production, 312, 127775. doi:10.1016/j.jclepro.2021.127775.

[57] Yoo, D. Y., You, I., & Zi, G. (2021). Effects of waste liquid–crystal display glass powder and fiber geometry on the mechanical properties of ultra-high-performance concrete. Construction and Building Materials, 266, 120938. doi:10.1016/j.conbuildmat.2020.120938.

[58] Abdellatief, M., AL-Tam, S. M., Elemam, W. E., Alanazi, H., Elgendy, G. M., & Tahwia, A. M. (2023). Development of ultra-high-performance concrete with low environmental impact integrated with metakaolin and industrial wastes. Case Studies in Construction Materials, 18, 1724. doi:10.1016/j.cscm.2022.e01724.

[59] Yu, L., & Wu, R. (2020). Using graphene oxide to improve the properties of ultra-high-performance concrete with fine recycled aggregate. Construction and Building Materials, 259, 120657. doi:10.1016/j.conbuildmat.2020.120657.

[60] Liu, T., Wei, H., Zou, D., Zhou, A., & Jian, H. (2020). Utilization of waste cathode ray tube funnel glass for ultra-high performance concrete. Journal of Cleaner Production, 249, 119333. doi:10.1016/j.jclepro.2019.119333.

[61] Suzuki, M., Seddik Meddah, M., & Sato, R. (2009). Use of porous ceramic waste aggregates for internal curing of high-performance concrete. Cement and Concrete Research, 39(5), 373–381. doi:10.1016/j.cemconres.2009.01.007.

[62] Afshinnia, K., & Rangaraju, P. R. (2016). Impact of combined use of ground glass powder and crushed glass aggregate on selected properties of Portland cement concrete. Construction and Building Materials, 117, 263–272. doi:10.1016/j.conbuildmat.2016.04.072.

[63] Qian, D., Yu, R., Shui, Z., Sun, Y., Jiang, C., Zhou, F., Ding, M., Tong, X., & He, Y. (2020). A novel development of green ultra-high performance concrete (UHPC) based on appropriate application of recycled cementitious material. Journal of Cleaner Production, 261, 121231. doi:10.1016/j.jclepro.2020.121231.

[64] Faried, A. S., Mostafa, S. A., Tayeh, B. A., & Tawfik, T. A. (2021). Mechanical and durability properties of ultra-high performance concrete incorporated with various nano waste materials under different curing conditions. Journal of Building Engineering, 43, 102569. doi:10.1016/j.jobe.2021.102569.

[65] Leng, Y., Rui, Y., Zhonghe, S., Dingqiang, F., Jinnan, W., Yonghuan, Y., Qiqing, L., & Xiang, H. (2023). Development of an environmental Ultra-High Performance Concrete (UHPC) incorporating carbonated recycled coarse aggregate. Construction and Building Materials, 362, 129657. doi:10.1016/j.conbuildmat.2022.129657.

[66] Feng, J., Yang, F., & Qian, S. (2021). Improving the bond between polypropylene fiber and cement matrix by nano calcium carbonate modification. Construction and Building Materials, 269, 121249. doi:10.1016/j.conbuildmat.2020.121249.

[67] Shen, P., Sun, Y., Liu, S., Jiang, Y., Zheng, H., Xuan, D., Lu, J., & Poon, C. S. (2021). Synthesis of amorphous nano-silica from recycled concrete fines by two-step wet carbonation. Cement and Concrete Research, 147, 106526. doi:10.1016/j.cemconres.2021.106526.

[68] Esmaeili, J., & Oudah Al-Mwanes, A. (2021). A review: Properties of eco-friendly ultra-high-performance concrete incorporated with waste glass as a partial replacement for cement. Materials Today: Proceedings, 42, 1958–1965. doi:10.1016/j.matpr.2020.12.242.

[69] Balasubramanian, B., Gopala Krishna, G. V. T., Saraswathy, V., & Srinivasan, K. (2021). Experimental investigation on concrete partially replaced with waste glass powder and waste E-plastic. Construction and Building Materials, 278, 122400. doi:10.1016/j.conbuildmat.2021.122400.

[70] Elaqra, H. A., Haloub, M. A. A., & Rustom, R. N. (2019). Effect of new mixing method of glass powder as cement replacement on mechanical behavior of concrete. Construction and Building Materials, 203, 75–82. doi:10.1016/j.conbuildmat.2019.01.077.

[71] Shen, P., Lu, L., He, Y., Rao, M., Fu, Z., Wang, F., & Hu, S. (2018). Experimental investigation on the autogenous shrinkage of steam cured ultra-high performance concrete. Construction and Building Materials, 162, 512–522. doi:10.1016/j.conbuildmat.2017.11.172.

[72] Collepardi, S., Coppola, L., Troli, R., & Collepardi, M. (1997). Mechanical properties of modified reactive powder concrete. American Concrete Institute, ACI Special Publication, SP-173, 1–21. doi:10.14359/6175.

[73] Lee, N. K., Koh, K. T., Kim, M. O., & Ryu, G. S. (2018). Uncovering the role of micro silica in hydration of ultra-high performance concrete (UHPC). Cement and Concrete Research, 104, 68–79. doi:10.1016/j.cemconres.2017.11.002.

[74] Wu, Z., Khayat, K. H., & Shi, C. (2017). Effect of nano-SiO2 particles and curing time on development of fiber-matrix bond properties and microstructure of ultra-high strength concrete. Cement and Concrete Research, 95, 247–256. doi:10.1016/j.cemconres.2017.02.031.

[75] Ling, T. C., & Poon, C. S. (2012). A comparative study on the feasible use of recycled beverage and CRT funnel glass as fine aggregate in cement mortar. Journal of Cleaner Production, 29–30, 46–52. doi:10.1016/j.jclepro.2012.02.018.

[76] Zhao, H., Poon, C. S., & Ling, T. C. (2013). Utilizing recycled cathode ray tube funnel glass sand as river sand replacement in the high-density concrete. Journal of Cleaner Production, 51, 184–190. doi:10.1016/j.jclepro.2013.01.025.

[77] Sharma, U., Singh, L. P., Zhan, B., & Poon, C. S. (2019). Effect of particle size of nanosilica on microstructure of C-S-H and its impact on mechanical strength. Cement and Concrete Composites, 97, 312–321. doi:10.1016/j.cemconcomp.2019.01.007.

[78] Erdem, S., Dawson, A. R., & Thom, N. H. (2012). Impact load-induced micro-structural damage and micro-structure associated mechanical response of concrete made with different surface roughness and porosity aggregates. Cement and Concrete Research, 42(2), 291–305. doi:10.1016/j.cemconres.2011.09.015.

[79] Tahwia, A. M., Elgendy, G. M., & Amin, M. (2022). Mechanical properties of affordable and sustainable ultra-high-performance concrete. Case Studies in Construction Materials, 16, 1069. doi:10.1016/j.cscm.2022.e01069.

[80] Tahwia, A. M., El-Far, O., & Amin, M. (2022). Characteristics of sustainable high strength concrete incorporating eco-friendly materials. Innovative Infrastructure Solutions, 7(1), 1–13. doi:10.1007/s41062-021-00609-7.

[81] Jing, R., Liu, Y., & Yan, P. (2021). Uncovering the effect of fly ash cenospheres on the macroscopic properties and microstructure of ultra-high-performance concrete (UHPC). Construction and Building Materials, 286, 122977. doi:10.1016/j.conbuildmat.2021.122977.

[82] Liu, J., Shi, C., & Wu, Z. (2019). Hardening, microstructure, and shrinkage development of UHPC: A review. Journal of Asian Concrete Federation, 5(2), 1–19. doi:10.18702/acf.2019.12.5.2.1.

[83] Yalçınkaya, Ç., & Çopuroğlu, O. (2021). Hydration heat, strength and microstructure characteristics of UHPC containing blast furnace slag. Journal of Building Engineering, 34, 101915. doi:10.1016/j.jobe.2020.101915.

[84] Abdulkareem, O. M., Fraj, A. Ben, Bouasker, M., Khouchaf, L., & Khelidj, A. (2021). Microstructural investigation of slag-blended UHPC: The effects of slag content and chemical/thermal activation. Construction and Building Materials, 292, 123455. doi:10.1016/j.conbuildmat.2021.123455.